Cell Reports

Article

# SMC complexes are guarded by the SUMO protease Ulp2 against SUMO-chain-mediated turnover

## Graphical abstract

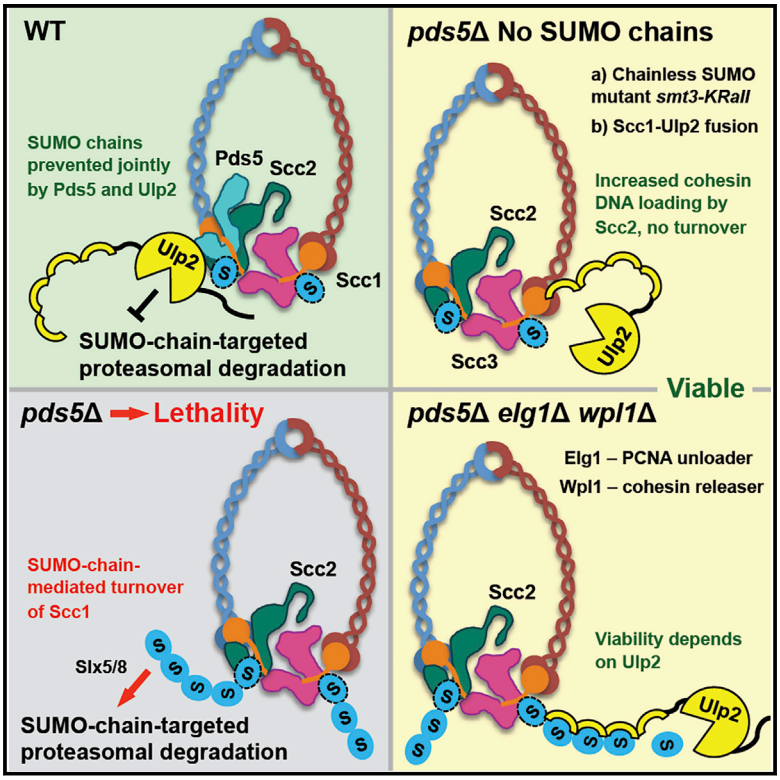


## Highlights

- SUMO chains target SMC complexes and are antagonized by the SUMO protease Ulp2
- Essential role of the cohesin regulatory subunit Pds5 is to counteract SUMO chains
- Fusion of Ulp2 to cohesin subunit kleisin Scc1 supports viability in the absence of Pds5
- Ulp2 curbs SUMO chain assembly, thus timing the turnover of the SMC complexes

## Authors

Ivan Psakhye, Dana Branzei

## Correspondence

dana.branzei@ifom.eu

## In brief

How the chromatin abundance of SMC complexes is regulated remains poorly understood. Psakhye and Branzei identify SUMO protease Ulp2 as a guardian of cohesin, condensin, and Smc5/6 complexes against SUMO-chain-targeted turnover. The authors show that the essential role of Pds5 cohesin subunit is to antagonize SUMO chains jointly with Ulp2.

Psakhye & Branzei, 2021, Cell Reports *36*, 109485
August 3, 2021 
https://doi.org/10.1016/j.celrep.2021.109485

CellPress

Cell Reports

CellPress
OPEN ACCESS

Article

# SMC complexes are guarded by the SUMO protease Ulp2 against SUMO-chain-mediated turnover

Ivan Psakhye[1] and Dana Branzei[1,2,3,*]
[1]IFOM, the FIRC Institute of Molecular Oncology, Via Adamello 16, 20139 Milan, Italy
[2]Istituto di Genetica Molecolare, Consiglio Nazionale delle Ricerche (IGM-CNR), Via Abbiategrasso 207, 27100 Pavia, Italy
[3]Lead contact
*Correspondence: dana.branzei@ifom.eu
https://doi.org/10.1016/j.celrep.2021.109485

## SUMMARY

Structural maintenance of chromosomes (SMCs) complexes, cohesin, condensin, and Smc5/6, are essential for viability and participate in multiple processes, including sister chromatid cohesion, chromosome condensation, and DNA repair. Here we show that SUMO chains target all three SMC complexes and are antagonized by the SUMO protease Ulp2 to prevent their turnover. We uncover that the essential role of the cohesin-associated subunit Pds5 is to counteract SUMO chains jointly with Ulp2. Importantly, fusion of Ulp2 to kleisin Scc1 supports viability of *PDS5* null cells and protects cohesin from proteasomal degradation mediated by the SUMO-targeted ubiquitin ligase Slx5/Slx8. The lethality of *PDS5*-deleted cells can also be bypassed by simultaneous loss of the proliferating cell nuclear antigen (PCNA) unloader, Elg1, and the cohesin releaser, Wpl1, but only when Ulp2 is functional. Condensin and Smc5/6 complex are similarly guarded by Ulp2 against unscheduled SUMO chain assembly, which we propose to time the availability of SMC complexes on chromatin.

## INTRODUCTION

Posttranslational modification of proteins with the small ubiquitin-like modifier (SUMO) is essential for eukaryotic cells because it regulates substrate fate by affecting protein interactions, activity, localization, and abundance (Flotho and Melchior, 2013). SUMOylation frequently targets entire protein groups, actively engaged in common functions (Jentsch and Psakhye, 2013; Psakhye and Jentsch, 2012), and fosters protein complex formation through SUMO binding to SUMO-interacting motifs (SIMs). Similar to ubiquitin, SUMO is conjugated to exposed lysines on the substrates leading to monoSUMOylation or, if several lysines are modified, to multiSUMOylation. Moreover, mono/multiSUMOylation may be extended to SUMO chains when lysines of SUMO conjugated to the substrate are being further modified with SUMO, leading to substrate polySUMOylation. The modifications are reversible and counteracted by SUMO proteases, which have different localization, substrate, and SUMO-linkage specificities (Hickey et al., 2012). In budding yeast, the SUMO protease Ulp2 has preference for SUMO chains and prevents substrate polySUMOylation, which can be further recognized by ubiquitin E3 ligases containing multiple SIMs. These so-called SUMO-targeted ubiquitin ligases (STUbLs) can mediate proteolytic or non-proteolytic ubiquitylation of the SUMOylated substrate (Sriramachandran and Dohmen, 2014). Thus, SUMO chains may function as a countdown timer if they are assembled on STUbL substrates.

We recently reported that SUMO-chain/Ulp2-protease-regulated proteasomal degradation is a mechanism that times the availability of the Dbf4-dependent kinase (DDK), a key replication initiation regulator (Psakhye et al., 2019). To extend our findings beyond DNA replication, we performed an unbiased SILAC (stable isotope labeling by amino acids in cell culture)-based proteomic screen to uncover degradation-prone SUMO conjugates that decrease in abundance in the absence of Ulp2 specifically in a SUMO-chain-dependent manner. Strikingly, we found subunits of all three structural maintenance of chromosomes (SMC) complexes, cohesin, condensin, and Smc5/6 (Nasmyth and Haering, 2005; Yatskevich et al., 2019), as potential hits, suggesting that the abundance of SMC complexes is regulated via a SUMO-chain-dependent mechanism.

Cohesin was previously shown to become SUMOylated upon loading onto DNA, and loss of cohesin SUMOylation resulted in cohesion defects (Almedawar et al., 2012; McAleenan et al., 2012). Moreover, the cohesin-associated factor, Pds5, was proposed to protect monoSUMOylated cohesin and facilitate cohesion by preventing via a yet unidentified mechanism Siz2 SUMO-ligase-mediated cohesin polySUMOylation that leads to increased Slx5/8 STUbL-mediated proteasome degradation of the cohesin kleisin, Scc1 (D'Ambrosio and Lavoie, 2014). More recently, depletion of *SENP6*, the human ortholog of Ulp2, was shown to decrease cohesin binding to chromatin and cause cohesion defects (Wagner et al., 2019). Taken together, these data suggest that mono/multiSUMOylation of DNA-loaded

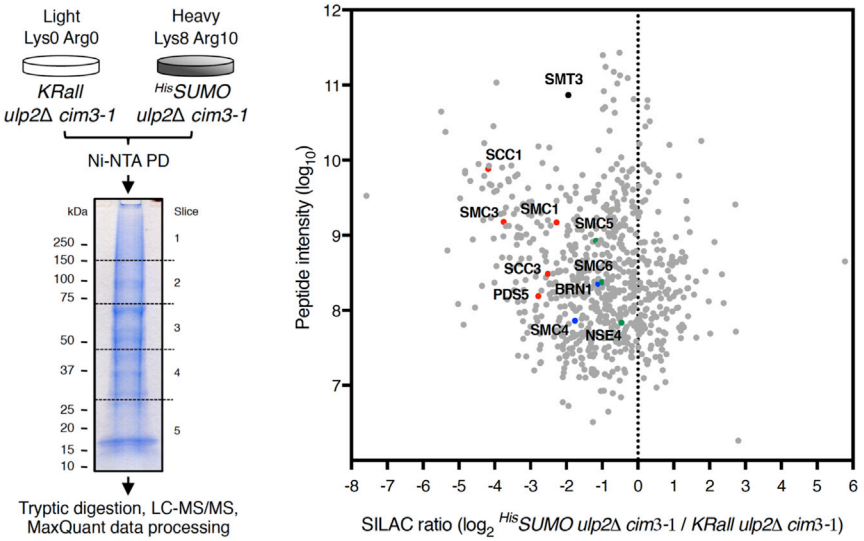


**Figure 1. SUMO chains promote the turnover of SUMOylated SMC complex subunits in the absence of Ulp2 SUMO protease**

Outline of SILAC experiment performed to detect degradation-prone SUMOylated substrates that decrease in abundance in a SUMO-chain-dependent manner in *ulp2Δ cim3-1* cells (left). SILAC ratios for 726 quantified proteins plotted against the sum of the relevant peptide intensities (right). SUMOylated subunits of cohesin (red), condensin (blue), and the Smc5/6 complex (green) accumulate if instead of $^{His}$SUMO, which is able to form SUMO chains, a lysine-less SUMO variant (*KRall*) that cannot form lysine-linked SUMO chains is expressed as the only source of SUMO.
See also Figure S1.

cohesin is important for cohesion, whereas polySUMOylation induced in *pds5* mutants targets cohesin for STUbL-mediated proteasomal turnover compromising cohesion.

Here we aimed to address if and how Ulp2 protects cohesin and other SMC complexes from SUMO-chain-targeted turnover. We find that fusion of Ulp2 to the cohesin's kleisin Scc1 protects cohesin from proteasomal degradation and supports viability in the complete absence of Pds5 that is otherwise essential. Moreover, we identify that simultaneous loss of the proliferating cell nuclear antigen (PCNA) unloader, Elg1, and the cohesin releaser, Wpl1, allows viability of *PDS5* null cells in a manner strictly depending on Ulp2 function. These results indicate that the essential function of Pds5 is to counteract SUMO chains jointly with Ulp2 rather than support cohesin activity in other direct ways. Condensin and Smc5/6 are also safeguarded by Ulp2 against unscheduled SUMO chain assembly, overall suggesting a SUMO-chain/Ulp2-protease-governed mechanism that instructs SMC complexes availability on chromatin.

## RESULTS

### SUMO chains target SMC complexes and promote their turnover

We have used quantitative proteomics to identify SUMO substrates whose turnover is promoted by SUMO chains in the absence of the SUMO protease Ulp2 that possesses SUMO-chain-editing activity in yeast cells (Eckhoff and Dohmen, 2015). To these ends, we used a SILAC-based mass spectrometry approach (Mann, 2006) and compared by denaturing Ni-NTA pull-down (Ni PD) (Psakhye and Jentsch, 2012, 2016) the levels of SUMO conjugates in *ulp2Δ cim3-1* mutants expressing either endogenous yeast SUMO (*SMT3*) N-terminally tagged with a 7xHis-tag ($^{His}$SUMO) or a lysine-less SUMO variant (*KRall*) that cannot form lysine-linked polySUMO chains (Figure 1, left). We used the temperature-sensitive proteasome-defective *cim3-1* mutant cells at the permissive temperature of 30°C to allow cell-cycle progression and accumulation of degradation-prone substrates, thus facilitating their identification by mass spectrometry. The SILAC screen quantified 726 potential SUMO conjugates (Figure 1, right); the abundance of most of them did not change significantly, while SUMO conjugates (Smt3) pulled down from the *KRall* mutant were more abundant in general. Notably, among the SUMO substrates strongly enriched in the sample derived from chainless SUMO *ulp2Δ cim3-1* cells were subunits of all three SMC complexes. SUMOylated cohesin subunits Smc1, Smc3, Scc1, Scc3, and Pds5 were enriched the most when SUMO chain growth was prevented by the *KRall* mutation, whereas SUMOylated condensin subunits Smc4 and Brn1 and the Smc5/6 complex subunits Smc5, Smc6, and Nse4 accumulated to a lesser extent.

Cohesin shows strong ties to the SUMO system (Almedawar et al., 2012; D'Ambrosio and Lavoie, 2014; McAleenan et al., 2012; Potts et al., 2006; Takahashi et al., 2008; Wu et al., 2012). Its regulatory subunit Pds5 is a known SUMO target (Stead et al., 2003) (Figure S1A) and is one of the first identified substrates of Ulp2 (Stead et al., 2003). These findings, together with the results of our SILAC screen suggesting that most of the cohesin subunits are subjected to SUMO-chain-mediated turnover, prompted us to focus on studying the regulation of the cohesin complex by SUMO chains and Ulp2.

We hypothesized that one of the roles of the essential regulatory cohesin subunit Pds5 is to recruit Ulp2 to protect cohesin against unscheduled SUMO-chain-mediated turnover. Indeed, we could confirm the interaction of Ulp2 with Pds5 using both co-immunoprecipitation (coIP) and yeast two-hybrid (Y2H) studies (Figures S1B–S1D). For the coIP, we C-terminally tagged endogenous Pds5 and Ulp2 with 13Myc and 9PK tags, respectively. Immunoprecipitations (IPs) with the anti-PK (Figure S1B) and anti-Myc (Figure S1C) antibodies revealed that Ulp2 interacts with Pds5 and there is preference toward upshifted, potentially SUMO-modified forms of proteins. These slower-migrating species of Pds5 and Ulp2 were coIPed with specific antibodies, but not mouse IgG (Figures S1B and S1C). For the Y2H studies, we used Gal4 DNA-binding domain (BD) fusions of various Pds5 truncations and the Gal4 activation domain (AD) fusion of catalytically dead Ulp2 (Ulp2-C624S;

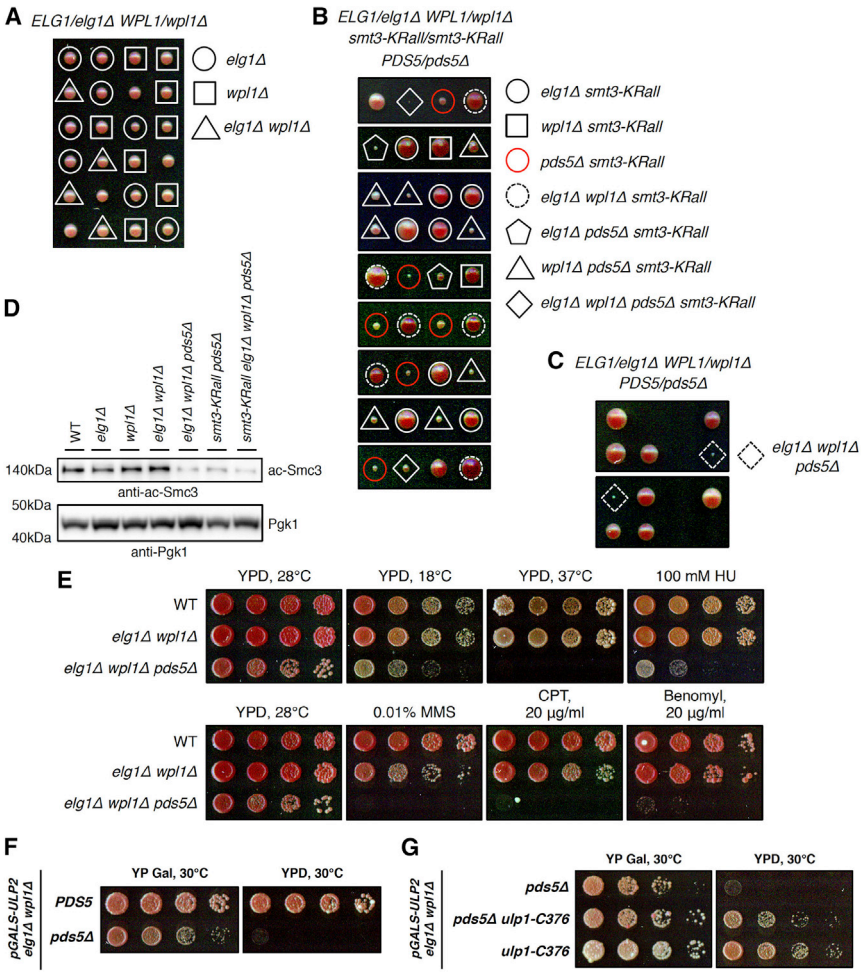


**Figure 2. The essential role of cohesin-associated subunit Pds5 is to counteract SUMO chains and is bypassed in the *elg1*Δ *wpl1*Δ background**

(A) Tetrad dissection analysis of *ELG1/elg1*Δ *WPL1/wpl1*Δ double mutant revealed no negative genetic interaction compared with WT.

(B) Lethality of *pds5*Δ cells is suppressed by chainless SUMO mutant *smt3-KRall*.

(C) Lethality of *pds5*Δ cells is bypassed in *elg1*Δ *wpl1*Δ background.

(D) Smc3 lysine K112, K113 acetylation is decreased (in three independent experiments) in *pds5*Δ cells, the lethality of which is suppressed either by *smt3-KRall*, *elg1*Δ *wpl1*Δ, or their combination.

(E) *pds5*Δ *elg1*Δ *wpl1*Δ cells are slow growth and exhibit sensitivity to temperature, HU, MMS, CPT, and benomyl.

(F) Viability of *pds5*Δ *elg1*Δ *wpl1*Δ cells depends on *ULP2* transcription.

(G) Lethality of *pds5*Δ *elg1*Δ *wpl1*Δ *ulp2* cells is bypassed by the spontaneous suppressor of *ulp2*Δ phenotypes *ulp1-C376*.

See also Figures S2 and S3.

Ulp2$_{CD}$), which we expected to interact stronger with potential substrates based on previous work on Ulp1$_{CD}$ that behaved like a SUMO substrate trap (Elmore et al., 2011) (Figures S1D–S1F). We observed weak Y2H interaction of Ulp2 with both N-terminal (amino acids [aa] 1–701) and C-terminal (aa 702–1277) fragments of Pds5 (Figure S1D). However, analysis of further N-terminal Pds5 truncations revealed auto-activation of the *HIS3* reporter gene by Pds5 N terminus (aa 1–250; Figure S1E), suggesting that binding of Ulp2 to Pds5 may be mediated by its C terminus. Indeed, using C-terminal truncations of Pds5, we found that the C-terminal fragment of Pds5 (aa 1,078–1,277) is required for the interaction with Ulp2 in the Y2H system (Figure S1F). Altogether, these results potentially support the notion that Pds5 recruits Ulp2 to prevent SUMO-chain-mediated turnover of cohesin.

## The essential role of Pds5 relates to curbing down SUMO chains

Cohesin plays critical roles in numerous cellular pathways (Dorsett, 2011; Losada, 2014; Nasmyth and Haering, 2009; Yatskevich et al., 2019), including sister chromatid cohesion and chromosome condensation, for both of which *PDS5* is required (Hartman et al., 2000; Panizza et al., 2000). Interestingly, sister chromatid cohesion defects and lethality of the temperature-sensitive *pds5-1* mutant are suppressed by deletion of *ELG1* (Tong and Skibbens, 2015), which acts in the context of the Elg1-Rfc2-5 complex as principal unloader of chromatin-bound PCNA (Kubota et al., 2013). Chromosome condensation defects of *pds5-1* mutant, but not lethality, are in turn suppressed by deletion of *RAD61* (*WPL1*) (Tong and Skibbens, 2015), which encodes the cohesin release factor WAPL that interacts with Pds5 and destabilizes cohesin's binding to DNA (Kueng et al., 2006).

To study the potential role of Pds5 in counteracting SUMO chains via Ulp2 recruitment to cohesin, we decided to examine the effect of *elg1*Δ and *wpl1*Δ mutations on the viability of *PDS5* null cells when SUMO chain formation is prevented. First, we confirmed that *elg1*Δ *wpl1*Δ double mutant does not affect cell growth compared with single mutants and wild-type (WT) cells (Figure 2A) (Maradeo and Skibbens, 2010). Then, we generated *ELG1/elg1*Δ *WPL1/wpl1*Δ *PDS5/pds5*Δ *smt3-KRall/smt3-KRall* diploid strain expressing chainless SUMO variant *smt3-KRall* as the only source of SUMO. The analysis of resulting haploids after sporulation and tetrad dissection of this strain should reveal if *elg1*Δ *wpl1*Δ *smt3-KRall* triple-mutant bypasses the essential role(s) of *PDS5*. Strikingly, we found that not only *pds5*Δ *elg1*Δ *wpl1*Δ *smt3-KRall* quadruple mutant was viable but also that expression of *smt3-KRall* alone bypassed the requirement of *PDS5* for viability (Figure 2B). We next analyzed if *elg1*Δ *wpl1*Δ *pds5*Δ triple mutant is viable following tetrad dissection of *ELG1/elg1*Δ *WPL1/wpl1*Δ *PDS5/pds5*Δ diploid strain. Interestingly, also the *elg1*Δ *wpl1*Δ double mutant suppressed the lethality of *pds5*Δ cells (Figure 2C). Thus, we

uncovered that the essential role of *PDS5* in budding yeast is linked to counteracting SUMO chains, and we identified a genetic background, *elg1*Δ *wpl1*Δ, in which this essential function is bypassed.

Next, we checked if expression of the chainless SUMO variant *smt3-KRall, elg1*Δ *wpl1*Δ double mutation, or their combination, is able to suppress the loss of another cohesin HAWK (HEAT-repeat proteins associated with kleisins) protein Scc3, which is required for cohesin binding to DNA (Li et al., 2018), but not for its loading to chromatin mediated by the Scc2/Scc4 complex (Ciosk et al., 2000). None of the mutations provided viability to *scc3*Δ haploids upon tetrad dissection of *ELG1/elg1*Δ *WPL1/wpl1*Δ *SCC3/scc3*Δ *smt3-KRall/smt3-KRall* diploid strain (Figure S2A). The lethality of cells upon deletion of *ECO1*, the acetyltransferase required for Smc3 lysine K112, K113 acetylation, and sister chromatid cohesion establishment (Rolef Ben-Shahar et al., 2008; Unal et al., 2008), is also not suppressed by expressing *smt3-KRall* and is only bypassed by *wpl1*Δ (Figure S2B). Thus, although *PDS5* overexpression partially suppresses the temperature sensitivity of certain *eco1*-thermosensitive mutants (Noble et al., 2006), *smt3-KRall* that bypasses the essential role of *PDS5* does not restore viability of cells lacking Eco1 (Figure S2B), suggesting that other functions of *PDS5* are required for this suppression.

To determine the consequences of *PDS5* loss for the chromatin-bound cohesin levels, we assessed Eco1-mediated Smc3 lysine K112, K113 acetylation in the identified *PDS5* null bypass conditions. Eco1 acetyltransferase targets cohesin loaded onto DNA (Ladurner et al., 2014), thus making Smc3 acetylation a good indicator of the functionally engaged cohesin amounts operating in the cell. To this end, we utilized a monoclonal antibody specific for the Eco1-mediated Smc3 lysine K112, K113 acetylation (Borges et al., 2010) and found that it was largely reduced, but not abolished, in all *pds5*Δ mutants (Figure 2D; Figure S2C). Thus, cells lacking Pds5 have reduced levels of chromatin-bound cohesin available to fulfill its functions, which is in agreement with findings in *pds5-ts* cells (D'Ambrosio and Lavoie, 2014; Panizza et al., 2000). We further found that although limited amounts of chromatin-bound acetylated cohesin in *pds5*Δ *elg1*Δ *wpl1*Δ mutants are sufficient to support viability, the mutant cells are sensitive to low and high temperatures, replication stress induced by hydroxyurea (HU), exposures to the DNA-alkylating agent methyl methanesulfonate (MMS), topoisomerase poison camptothecin (CPT), and microtubule-depolymerizing drug benomyl (Figure 2E).

Loss of *WPL1* was previously reported to cause an increase in pericentromeric cohesin in cells blocked in late G1 by the Cdk1 inhibitor Sic1, whereas *wpl1*Δ had little or no effect on the extent of Scc1 association with chromosome arms (Petela et al., 2018). To provide insights on how *elg1*Δ *wpl1*Δ mutant suppresses the lethality of *pds5*Δ cells, we next analyzed the cohesin levels on chromatin at the pericentromeric region of *CEN10*, *TER1004*, and the centromere-distal region on chromosome 3, *ARS305*, by performing chromatin immunoprecipitation (ChIP) of C-terminally 6HA-tagged Scc1 from nocodazole-arrested WT, *wpl1*Δ, *elg1*Δ *wpl1*Δ, and *elg1*Δ *wpl1*Δ *pds5*Δ cells (Figures S2D and S2E). Interestingly, we observed s statistically significant increase of Scc1 association in *wpl1*Δ and *elg1*Δ *wpl1*Δ mutants compared with WT specifically at the pericentromeric region (Figure S2D), but not at the chromosome arm (Figure S2E). Depletion of Pds5 using an auxin-inducible degron system in G1-arrested cells was shown previously to increase genome-wide Scc1 chromatin association 2-fold (Petela et al., 2018). The authors suggested that Pds5 negatively regulates Scc2-mediated cohesin loading throughout the genome. In line with their findings, we observed a 2-fold increase in Scc1 chromatin levels at the centromere-distal region in nocodazole-arrested *elg1*Δ *wpl1*Δ *pds5*Δ mutant compared with WT and *elg1*Δ *wpl1*Δ cells (Figure S2E). Scc1 chromatin levels at the pericentromeric region in the *elg1*Δ *wpl1*Δ *pds5*Δ were also increased at least 2-fold compared with WT; however, no further increase was observed compared with *elg1*Δ *wpl1*Δ double mutant (Figure S2D). Elevated Scc1 chromatin loading mediated by Scc2 in the absence of Pds5 as assessed by ChIP does not, however, provide information regarding the fate of the loaded cohesin complexes, which may be targeted by subsequent SUMO-chain-mediated turnover in *PDS5* null cells causing a major reduction of Eco1-mediated Smc3 acetylation levels (Figure 2D; Figure S2C). To examine the overall amounts of Scc1 enriched on chromatin in the absence of Pds5, we next performed chromatin fractionation and found that both chromatin-bound Scc1 and Smc3 lysine K112, K113 acetylation levels were reduced in the *elg1*Δ *wpl1*Δ *pds5*Δ and *pds5*Δ *smt3-KRall* cells (Figure S2F).

## Ulp2 protease is essential in *pds5*Δ *elg1*Δ *wpl1*Δ cells, and its loss is bypassed by a spontaneous suppressor of *ulp2*Δ

How the *elg1*Δ *wpl1*Δ double mutant bypasses the essential role of *PDS5* in counteracting SUMO chains is unclear, but we speculated that the viability of *pds5*Δ *elg1*Δ *wpl1*Δ triple mutant may depend on the presence of the Ulp2 protease as the only source of SUMO-chain-editing activity in yeast cells. To test our hypothesis, we replaced the endogenous promoter of *ULP2* with the galactose-inducible *GAL* promoter, whose transcription can be inhibited by shifting cells from galactose-containing YP Gal to glucose-containing YPD (yeast extract-peptone-dextrose) media. Importantly, upon transcriptional *ULP2* shut-off, the *elg1*Δ *wpl1*Δ *pds5*Δ mutant lost viability, whereas *elg1*Δ *wpl1*Δ *PDS5* cells were not affected (Figure 2F). Furthermore, the lethality of *elg1*Δ *wpl1*Δ *pds5*Δ mutant following Ulp2 depletion could be suppressed by a spontaneous suppressor of *ulp2*Δ phenotypes that we identified and denoted as *ulp1-C376* (Figure 2G), as described below (Figure S3).

Cells lacking Ulp2 exhibit a pleiotropic phenotype that includes temperature sensitivity and increased sensitivity to HU (Li and Hochstrasser, 2000). We performed a screen for spontaneous suppressors of *ulp2*Δ-associated HU sensitivity and isolated five suppressors that also alleviated the temperature sensitivity (Figure S3A). Backcrossing isolated suppressors to the *ulp2*Δ mutant of the opposite mating type revealed $2^{+}$:$2^{-}$ segregation of the HU sensitivity (Figure S3B), which points to a single mutated gene locus responsible for the suppression. Whole-genome sequencing (WGS) of the isolated suppressors led to the identification of a single point mutation on chromosome 16 at the *YPL020C* (*ULP1*) gene in all five suppressors,

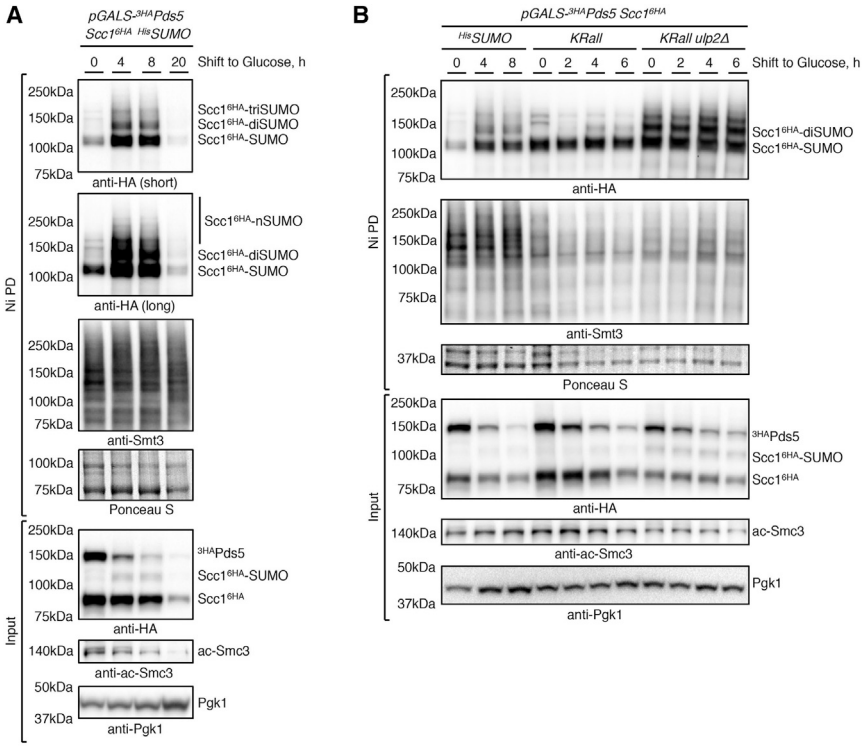


**Figure 3. Loss of Pds5 triggers SUMOylation of cohesin's kleisin Scc1 that is counteracted by Ulp2**

(A) Loss of Pds5 triggers SUMOylation of cohesin's kleisin Scc1 and leads to the reduction of its protein levels, as well as of Smc3 lysine K112, K113 acetylation levels (in three independent experiments). Denaturing Ni-NTA pull-down (Ni PD) was performed to isolate $^{His}$SUMO conjugates from cells expressing C-terminally 6HA-tagged Scc1 at endogenous levels and N-terminally 3HA-tagged Pds5 under the control of inducible *GAL* promoter. Cells were collected at the indicated time after shift from galactose- to glucose-containing media. Ni PD efficiency was assayed using anti-Smt3 antibody and Ponceau S staining. Pgk1 served as loading control.

(B) Expression of a lysine-less SUMO variant *KRall* that cannot form lysine-linked SUMO chains instead of $^{His}$SUMO results in the accumulation of monoSUMOylated Scc1 species even prior to *PDS5* shut-off. Loss of Ulp2 leads to further increase in Scc1 multiSUMOylation (in two independent experiments).

See also Figure S4.

but not in WT or *ulp2*Δ cells (Figure S3C). Ulp1 is the second yeast SUMO protease besides Ulp2. Differently from Ulp2, it does not have preference for SUMO chains, is essential for the maturation of conjugatable SUMO from its precursor polypeptide, and is anchored to nuclear pore complexes (NPCs) via its N terminus (Li and Hochstrasser, 1999, 2000, 2003; Mossessova and Lima, 2000; Panse et al., 2003). Re-sequencing of the *ULP1* locus validated the WGS results and confirmed a single insertion c.741_742insA denoted as *ulp1-sup* (Figure S3D). This insertion results in a frameshift predicted to generate a C-terminally truncated Ulp1 variant p.Val248Serfs*7 lacking the protease domain (Figure S3E), a notion not consistent with the essential nature of Ulp1 and its protease domain (Figures S3F and S3G) and different from the isolated *ulp1-sup* (Figures S3H and S3I). Careful analysis of the *ULP1* sequence revealed an alternative transcription/translation start site upstream of the frameshift mutation that might be used in *ulp1-sup* causing the expression of an N-terminally truncated Ulp1 variant (Figure S3I) with a new N-terminal extension of 7 aa upstream of Lys246 (Figure S3J). To confirm that *ulp1-sup* is indeed generating an N-terminally truncated Ulp1 variant able to suppress *ulp2*Δ phenotypes and provide viability as the only source of SUMO protease activity in the cell, we constructed the *ulp1-C376* mutant (Figure S3K). Specifically, we replaced *ulp1*Δ in *ULP2/ulp2*Δ *ULP1/ulp1*Δ diploid cells with *ulp1* sequence c.[741_742insA; 1_712del] that lacks the N-terminal NPC-targeting region (aa 1–245; first 712 nt of *ULP1* open reading frame (ORF) deleted). Tetrad dissection of the resulting *ULP2/ulp2*Δ *ULP1/ulp1-C376* diploids (Figure S3L) revealed that *ulp1-C376* suppressed the HU and temperature sensitivity of *ulp2*Δ cells similar to *ulp1-sup* (Figure S3M). Because Ulp1-C376 is expressed at very low levels from the alternative start site compared with WT Ulp1 (Figure S3I), it does not lead to cell death as a result of excessive deSUMOylation observed upon expression of N-terminal Ulp1 truncations at higher levels (Li and Hochstrasser, 2003; Mossessova and Lima, 2000).

Taken together, the identified spontaneous suppressor of *ulp2*Δ phenotypes *ulp1-C376* is the N-terminal truncation of Ulp1 that is no longer tethered to the NPC and is able to deSUMOylate Ulp2 substrates in the nucleoplasm providing viability to the otherwise lethal *elg1*Δ *wpl1*Δ *pds5*Δ *ulp2* quadruple mutant (Figure 2G). Thus, the viability of *pds5*Δ *elg1*Δ *wpl1*Δ cells depends on Ulp2 ability to counteract SUMO chains and can be bypassed by inducing limited deSUMOylation with the *ulp1-C376* suppressor of *ulp2* phenotypes.

## Loss of Pds5 triggers SUMOylation of cohesin's kleisin Scc1 that is counteracted by Ulp2

We showed that SUMOylated cohesin subunits are targeted by SUMO chains for turnover in the absence of Ulp2 (Figure 1), that the cohesin's regulatory subunit Pds5 is no longer essential when SUMO chains cannot form (Figure 2B), and that *pds5*Δ *elg1*Δ *wpl1*Δ cells rely on Ulp2 activity or may survive when N-terminal Ulp1 truncation not tethered to the NPC can perform Ulp2 functions (Figures 2F and 2G). Next, we aimed to address whether Ulp2 together with Pds5 indeed protects SUMOylated cohesin from SUMO-chain-mediated turnover.

In line with previous observations in a *pds5-1* mutant (D'Ambrosio and Lavoie, 2014), we find that the lethality caused by transcriptional *PDS5* shut-off is suppressed by *slx5*Δ and expression of the chainless SUMO *smt3-KRall* variant (Figure S4A). Importantly, conditional depletion of Pds5 expressed

under the *GAL* promoter allowed us to follow the induction of cohesin SUMOylation and turnover (Figure 3A) by monitoring SUMO modification of cohesin's kleisin Scc1 and its Slx5/8-targeted proteasome-mediated degradation, previously shown to be enhanced in *pds5-1* (D'Ambrosio and Lavoie, 2014). Scc1 monoSUMOylation is detected at low levels prior to *PDS5* shut-off (induced by shift to glucose-containing YPD media) in cells expressing $^{His}$SUMO able to form chains (Figure 3A). Four-eight hours after the shift to YPD, Pds5 levels drop, whereas monoSUMOylated Scc1 species massively accumulate and di/triSUMO-modified Scc1 can be detected. Pds5 depletion is accompanied by reduction in Smc3 lysine K112, K113 acetylation levels and degradation of the unmodified chromatin-bound Scc1 (Figure 3A, Input; Figure S4B), which is hardly detected 20 h after *PDS5* shut-off and leads to loss of its SUMOylation. Importantly, expression of the chainless SUMO variant *KRall* results in accumulation of monoSUMOylated Scc1 species even prior to Pds5 depletion (Figure 3B, compare time point 0 in *KRall* versus $^{His}$SUMO background), suggesting that when SUMO chain formation is prevented, monoSUMOylated Scc1 species become more stable. Moreover, deletion of *ULP2* in the *KRall* background leads to further accumulation of monoSUMOylated Scc1 species now readily detectable also in the inputs and accompanied by increase in di/triSUMO-modified Scc1 species (Figure 3B, *KRall ulp2*Δ background). The latter suggests that Ulp2 is able to either cleave off SUMO of mono/multiSUMOylated Scc1, or that physical interaction of Ulp2 with cohesin prevents Scc1 SUMOylation, similar to what has been proposed for Pds5 (D'Ambrosio and Lavoie, 2014). Because expression of the catalytically inactive *ulp2-C624S* mutant results in similar Scc1 multi-SUMOylation levels as observed in *ulp2*Δ mutant (Figure S4C), we conclude that Ulp2 is able to cleave off SUMO of mono/multi-SUMOylated Scc1. Notably, when SUMO chains are able to form ($^{His}$SUMO expressed), the contribution of Ulp2 to the protection of monoSUMOylated Scc1 species is hardly visible in Ni PD and is manifested by the accumulation of diSUMOylated Scc1 species in *ulp2*Δ cells (Figure S4D), in contrast with the *KRall* background (Figure 3B, compare time point 0 in *KRall* versus *KRall ulp2*Δ) where mono/multiSUMOylated Scc1 species are no longer converted to the degradation-prone polySUMOylated species and accumulate. Taken together, these data reveal a role for Ulp2 in guarding mono/multiSUMOylated Scc1 species of cohesin against SUMO-chain-mediated proteasomal turnover that is induced upon Pds5 loss.

## Fusion of Ulp2 to Scc1 supports viability in the absence of Pds5 and protects cohesin from SUMO-chain-mediated turnover

To unambiguously probe whether Ulp2 guards cohesin against SUMO-chain-targeted proteasomal degradation, we next asked if fusion of Ulp2 to the cohesin's kleisin Scc1 can suppress the lethality of cells lacking Pds5. Previously, fusion of the catalytically active Ulp1 domain to Scc1 (Scc1-UD) was shown to promote loss of cohesin's SUMO modifications, including mono-SUMOylation of Smc3 and Scc1-UD itself (Almedawar et al., 2012). Scc1-UD failed to complement the temperature-sensitive phenotype of *scc1-73* cells and showed sister chromatid cohesion defects, emphasizing the importance of cohesin SUMOylation for this process. Differently from Scc1-UD that abolishes cohesin SUMOylation, Ulp2 fusion to Scc1 should specifically antagonize its polySUMOylation in the absence of Pds5, leaving mono/multiSUMOylation intact and possibly stabilizing the kleisin.

To this end, we C-terminally fused the Ulp2 fragment (aa 1–734) to the endogenous Scc1 without any linker, providing Scc1-Ulp2 fusion *scc1-ulp2$_{734}$-6HA* as the only source of cohesin's kleisin in the cell (Figure 4A). The fused Ulp2 fragment contains N-terminal SIMs required for recognition of SUMO chains (Psakhye et al., 2019) and a protease domain but is lacking its C-terminal 300 aa where sequences that mediate its localization to the nucleolus and the inner kinetochore reside (Liang et al., 2017; Suhandynata et al., 2019). Additionally, we established catalytically dead *scc1-ulp2$_{734}$-C624S-6HA* fusion with Ulp2 active site cysteine mutated (Figure 4A) and *scc1-ulp2$_{734}$-sim-6HA* fusion having Ulp2 N-terminal SIMs required for robust SUMO-chain-binding mutated (Figure S5A).

First, we validated that expression of these fusions as the only source of cohesin's kleisin in WT cells supports viability, and that different fusions are expressed at similar levels (Figure S5B). Next, we confirmed that expression of the Ulp2 catalytically dead *scc1-ulp2$_{734}$-C624S-6HA* fusion in the *pds5*Δ *elg1*Δ *wpl1*Δ background is also tolerated (Figure S5C).

Importantly, catalytically active *scc1-ulp2$_{734}$-6HA*, but not catalytically dead *scc1-ulp2$_{734}$-C624S-6HA* or *scc1-ulp2$_{734}$-sim-6HA* fusion defective in binding to SUMO chains, was able to efficiently suppress the lethality of cells upon *PDS5* transcriptional shut-off (Figure 4B). Interestingly, if cells were allowed to grow longer on YPD plates, minor suppression of lethality induced by Pds5 depletion was also observed in cells expressing *scc1-ulp2$_{734}$-sim-6HA* fusion (Figure S5D), suggesting that when fused to Scc1, Ulp2 is able to antagonize polySUMOylation even when SUMO chain recognition is compromised. In the same line, *scc1-ulp2$_{734}$-6HA* fusion, but not catalytically dead *scc1-ulp2$_{734}$-C624S-6HA*, provided for viability of *pds5*Δ *elg1*Δ *wpl1*Δ cells upon glucose-induced transcriptional shut-off of *ULP2* (Figure 4C).

Finally, we followed the turnover of the Scc1-Ulp2 fusions in *pds5*Δ *elg1*Δ *wpl1*Δ cells upon *ULP2* shut-off and found that although the catalytically dead fusion is largely degraded 8 h after Ulp2 depletion (Figure 4D), the catalytically active fusion remains stable (Figure 4E).

Moreover, we followed the SUMOylation status of these fusions upon *ULP2* shut-off by performing Ni PD of $^{His}$SUMO conjugates able to form SUMO chains (Figures 5A and 5B). Catalytically active Scc1-Ulp2 fusion remained monoSUMOylated (Figure 5A, Ni PD), and Smc3 lysine K112, K113 acetylation levels did not change significantly upon depletion of Ulp2 (Figure 5A, Input). In contrast, catalytically dead Scc1-Ulp2 fusion became excessively SUMOylated after 4 h of Ulp2 depletion (Figure 5B, Ni PD); monoSUMOylated species were converted to slower-migrating polySUMOylated species and finally degraded resulting in the loss of unmodified Scc1-Ulp2 fusion after 8 and 20 h (Figure 5B, Input). Smc3 lysine K112, K113 acetylation levels were also largely reduced (Figure 5B), similar to the situation upon *PDS5* shut-off (Figure 3A). Taken together, these

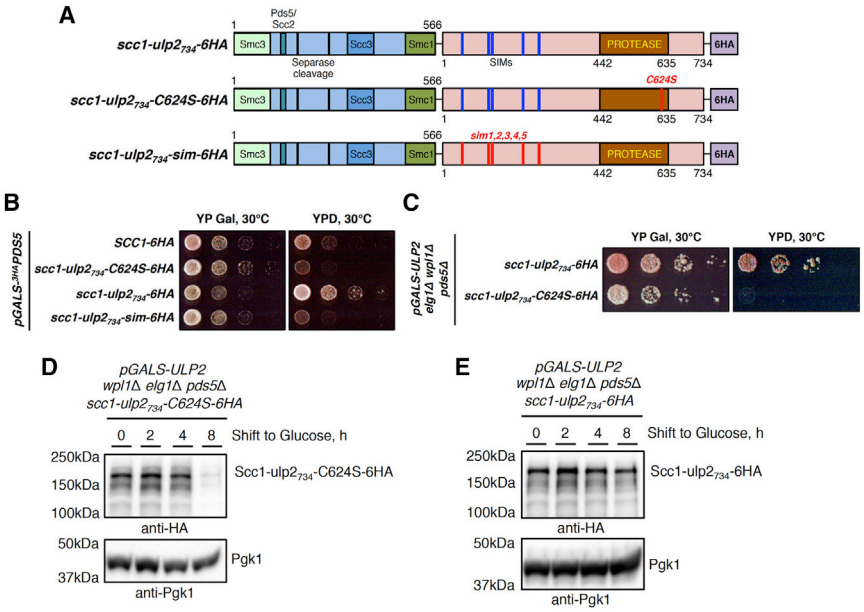


**Figure 4. Fusion of Ulp2 to cohesin's kleisin Scc1 supports viability in the absence of Pds5 and protects cohesin from turnover**

(A) Schematic representation of Scc1-Ulp2 fusions used in this study; fusion is the only source of cohesin's kleisin in the cell. Ulp2 fragment (aa 1–734) is fused C-terminally to endogenous Scc1. The N terminus of Ulp2 harbors five SIMs (colored blue) necessary for binding to SUMO chains and is followed by the protease domain; C terminus (aa 735–1,034) is replaced with 6HA tag. Catalytically active Ulp2 fusion to Scc1 is denoted *scc1-ulp2*$_{734}$*-6HA*, catalytically dead *scc1-ulp2*$_{734}$*-C624S-6HA* carries point mutation in active site, and *scc1-ulp2*$_{734}$*-sim-6HA* has all N-terminal SIMs mutated, losing ability to recognize SUMO chains.

(B) Catalytically active *scc1-ulp2*$_{734}$*-6HA* fusion supports viability upon *PDS5* shut-off, whereas *scc1-ulp2*$_{734}$*-C624S-6HA* and *scc1-ulp2*$_{734}$*-sim-6HA* fusions do not.

(C) Catalytically active *scc1-ulp2*$_{734}$*-6HA* fusion supports viability of *pds5Δ elg1Δ wpl1Δ* cells upon *ULP2* shut-off, whereas catalytically dead *scc1-ulp2*$_{734}$*-C624S-6HA* fusion does not.

(D and E) Upon *ULP2* shut-off in *elg1Δ wpl1Δ pds5Δ* background, the protein levels of the catalytically dead Scc1-ulp2$_{734}$-C624S-6HA fusion decrease (D), whereas catalytically active Scc1-ulp2$_{734}$-6HA fusion remains stable (E) in three independent experiments.
See also Figure S5.

experiments demonstrate that Ulp2 protects cohesin from SUMO-chain-mediated proteasomal turnover in collaboration with Pds5, and that the essential function of budding yeast Pds5 is to counteract SUMO chain targeting of cohesin, which can be bypassed either by expression of chainless SUMO variant (Figure 2B) or by the Ulp2 fusion to cohesin.

## Condensin is protected by Ulp2 against SUMO-chain-mediated turnover

Condensin subunits are known SUMO substrates (Takahashi et al., 2008); however, the functional significance of their modification is not clear. Recently, suppressor screening in fission yeast revealed that mutants of condensin's non-SMC subunits are rescued by impairing the SUMOylation pathway (Xu and Yanagida, 2019). Moreover, deleting *ULP2* was synthetically lethal with the fission yeast temperature-sensitive *cut3/smc4* mutant at permissive temperatures for *cut3-477*, while the *ulp2Δ* mutant showed defective chromosome condensation (Robellet et al., 2014).

In our SILAC-based proteomics screen, we identified condensin subunits Smc4 and Brn1 as potential substrates of SUMO-chain-targeted turnover in cells lacking Ulp2 (Figure 1). Furthermore, overexpression of *ULP2* was found to suppress the temperature sensitivity of the *smc2-6* mutant, while *ulp2Δ* cells were defective in enriching condensin on mitotic chromatin, in particular at rDNA (D'Amours et al., 2004; Strunnikov et al., 2001). We reasoned that similar to cohesin, the condensin complex may be guarded by Ulp2 against SUMO-chain-mediated turnover. We first used genetic analysis to strengthen our hypothesis. Although *ULP2* overexpression suppresses *smc2-6* (Strunnikov et al., 2001) and *smc2-8* (Stead et al., 2003) alleles, we found that *ulp2Δ* has synergistic growth defect with temperature-sensitive *smc2-8* mutant (Figure 6A) at temperatures permissive for the single mutants, similar to fission yeast *cut3/smc4* (Robellet et al., 2014), suggesting that in the absence of Ulp2, the function of condensin is further compromised in *smc2-8* cells. Importantly, the above-mentioned synthetic lethality of *smc2-8 ulp2Δ* cells is rescued by expressing as the single source of SUMO the *smt3-KRall* SUMO variant that cannot form lysine-linked SUMO chains (Figure 6B).

In cohesin, the lethality caused by depletion of the HAWK protein subunit Pds5 is suppressed by the expression of *smt3-KRall* (Figure 2B) and is accompanied by massive SUMOylation of cohesin's kleisin Scc1 (Figure 3). However, this was not the case when we conditionally depleted the essential HAWK proteins of condensin, Ycg1 and Ycs4, in the *smt3-KRall* background (Figure S6A), emphasizing that protection of condensin against SUMO chains is not their essential function. Furthermore, multiSUMOylation of condensin's kleisin Brn1 tagged C-terminally with 6HA slowly decreased following transcriptional shut-off of either *YCG1* (Figure S6B) or *YCS4* (Figure S6C), contrary to multiSUMOylation of cohesin's kleisin Scc1 upon Pds5 depletion (Figure 3A). Nevertheless, the synthetic lethality of *smc2-8 ulp2Δ* cells was suppressed by expressing *smt3-KRall* (Figure 6B) and deleting *SLX5* (Figure 6C; Figure S6D). Taken together, these genetic studies support a model in which Ulp2 guards condensin against SUMO-chain-targeted and Slx5/8 STUbL-mediated turnover. Corroborating this, loss of Ulp2 in cells expressing $^{His}$SUMO able to form chains resulted in the decrease of monoSUMOylated Brn1 species compared with WT cells detected by Ni PD, whereas expression of the chainless SUMO mutant *KRall* not only increased the abundance of monoSUMOylated Brn1 in WT cells but also suppressed the observed drop in *ulp2Δ* mutant (Figure 6D). However, monoSUMOylated

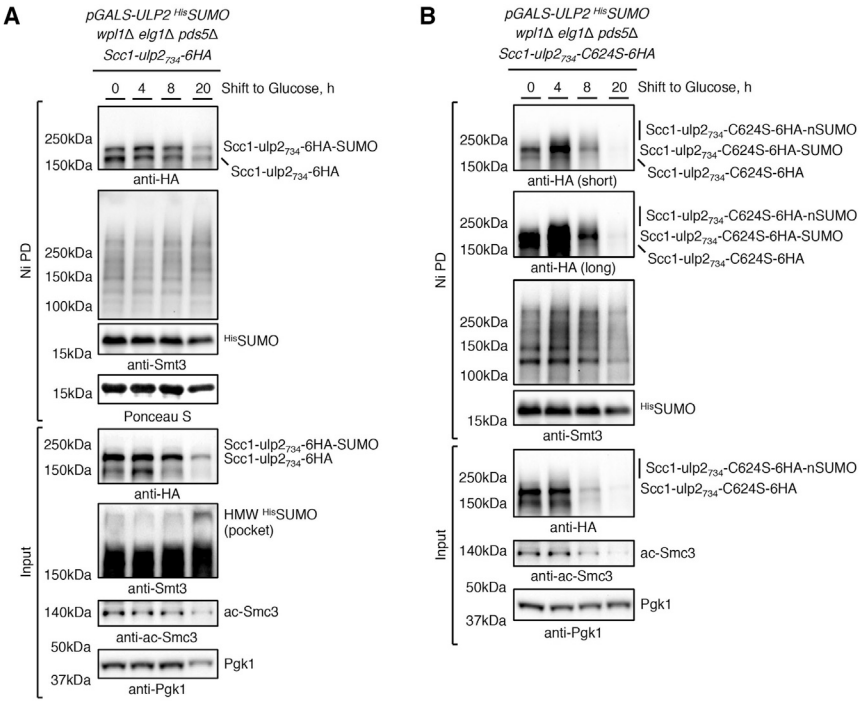


**Figure 5. Ulp2 fusion to cohesin's kleisin Scc1 keeps it in monoSUMOylated state and protects from SUMO-chain-targeted turnover**

(A and B) Catalytically active *scc1-ulp2$_{734}$-6HA* fusion maintains its protein and monoSUMOylation levels, as well as Smc3 lysine K112, K113 acetylation levels, upon *ULP2* shut-off in *pds5*Δ *elg1*Δ *wpl1*Δ cells, whereas catalytically dead *scc1-ulp2$_{734}$-C624S-6HA* fusion does not (in two independent experiments). Ni PD was performed to isolate $^{His}$SUMO conjugates from cells expressing either *scc1-ulp2$_{734}$-6HA* (A) or *scc1-ulp2$_{734}$-C624S-6HA* (B) and *ULP2* under the control of inducible *GAL* promoter. High-molecular-weight (HMW) polySUMO conjugates accumulate in input upon *ULP2* shut-off.

See also Figure S5.

Brn1 species are not particularly prone to proteasomal degradation, because they are not stabilized in the temperature-sensitive *cim3-1* proteasome-defective mutant (Figure S6E) grown at permissive temperature. Overall, the results suggest that in the absence of Ulp2, SUMO chains might target the condensin complex for disassembly and release from chromatin.

## The Smc5/6 complex is protected by Ulp2 against SUMO-chain-mediated turnover

We next studied if the third SMC complex Smc5/6 is similarly regulated. First, using a genetic approach, we found that *ulp2*Δ has synergistic growth defects with the temperature-sensitive *smc6-56* mutant (Figure 7A) at temperatures permissive for the single mutants, suggesting that in the absence of Ulp2, the function of the Smc5/6 complex is further compromised, similar to condensin (Figure 6A).

We then checked if expression of the chainless SUMO variant *smt3-KRall* is able to suppress either *smc6-56* or loss of the essential non-SMC element proteins Nse3 and Nse5. Neither the temperature sensitivity of *nse3-ts-12* and *smc6-56* mutants nor the lethality upon depletion of Nse5-AID using the auxin-inducible degron system (Nishimura et al., 2009) was suppressed by *smt3-KRall* (Figures S7A–S7C). Rather, we observed synthetic sick/lethal genetic interaction between *smc6-56* and *smt3-KRall* at temperatures permissive for the single mutants (Figure S7C). Previously, *smc6* mutations were shown to be synthetic sick/lethal with mutation of Sgs1 (Menolfi et al., 2015), whereas *sgs1*Δ cells require SUMO chain formation to survive and die upon expression of *smt3-KRall* (Mullen et al., 2011). Therefore, the synthetic lethality of *smc6-56 smt3-KRall* may be explained by the compromised function that is fulfilled by the Smc5/6 complex in collaboration with Sgs1 (Menolfi et al., 2015). The non-SMC element of the Smc5/6 complex Mms21 is a SUMO ligase that is responsible for Smc5/6 complex autoSUMOylation targeting primarily the Smc5 subunit (Zhao and Blobel, 2005). However, the Siz2 SUMO ligase also contributes to Smc5 SUMOylation (Bustard et al., 2016). Because we cannot use *smt3-KRall* to suppress the synthetic lethality of *smc6-56 ulp2*Δ double mutant, we checked if loss of Siz2 is able to do so. Previously, the temperature sensitivity of cohesin's *pds5-1* mutant was suppressed by *siz2*Δ (D'Ambrosio and Lavoie, 2014). We found the same to be true also for *smc6-56 ulp2*Δ (Figure 7B) and *smc6-P4 ulp2*Δ (Figure S7D) cells. Moreover, the synthetic growth defect of *smc6-P4 ulp2*Δ double mutant is suppressed by deletion of the STUbL subunit Slx5 (Figure S7E). In addition, *ulp2*Δ showed synthetic lethal/sick interactions with mutations in Esc2, Sgs1, and Rrm3 (Figures S7F–S7I), previously found to function jointly with Smc5/6 to facilitate processing of recombination intermediates (Esc2, Sgs1) (Branzei et al., 2006; Sollier et al., 2009) and replication through difficult-to-replicate regions (Rrm3) (Menolfi et al., 2015). Notably, these synthetic sick/lethal interactions could be suppressed by *siz2*Δ (Figures S7J and S7K), *ulp1-C376* (Figure S7L), and *slx5*Δ (Figure S7M). Taken together, these results suggest that also the Smc5/6 complex is negatively regulated by Siz2-mediated polySUMOylation, which, when not antagonized by Ulp2, is being recognized by the Slx5/8 STUbL and targets the complex for turnover.

In line with genetics, we found that monoSUMOylated species of Nse4, the kleisin of the Smc5/6 complex, accumulate in *slx5*Δ and decrease in abundance in *ulp2*Δ compared with WT cells (Figure 7C). Moreover, similar to condensin's kleisin Brn1 (Figure S6E), monoSUMOylated Nse4 species are not particularly prone to proteasomal degradation because they are not further enriched in *ulp2*Δ *cim3-1* mutant compared with *ulp2*Δ cells (Figure 7D). However, in Ni PD experiments, we find that monoSUMOylated Nse4 strongly accumulates in both WT and *ulp2*Δ when chainless SUMO variant *KRall* is expressed instead

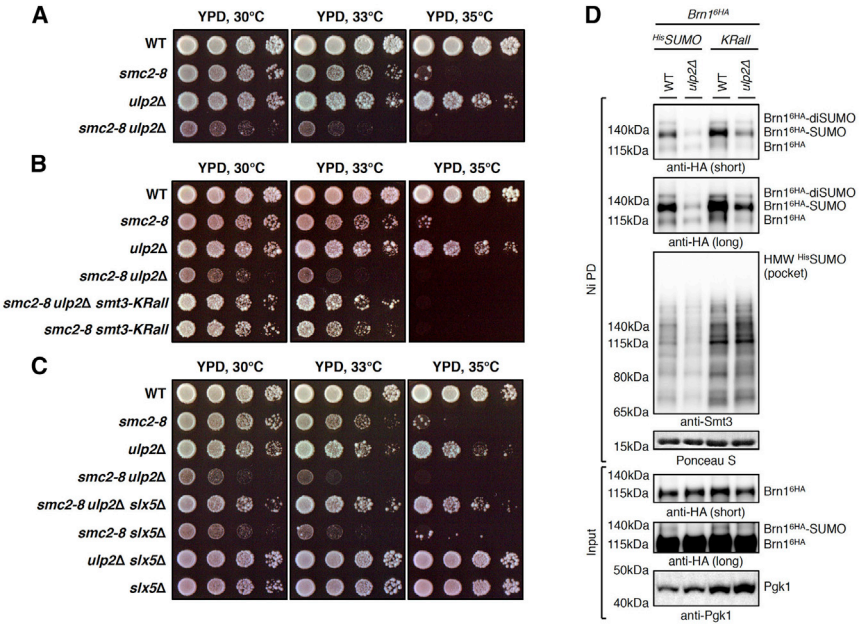


**Figure 6. Condensin is protected by Ulp2 against SUMO-chain-mediated turnover**

(A) Temperature-sensitive *smc2-8* mutant exhibits synthetic sick/lethal genetic interaction with *ulp2*Δ at permissive temperatures for *smc2-8* cells.

(B and C) Synthetic lethality of *smc2-8 ulp2*Δ cells at permissive temperatures for *smc2-8* single mutant is suppressed if a chainless SUMO variant *smt3-KRall* is expressed as the only source of SUMO (B) or if STUbL subunit Slx5 is deleted (C).

(D) Levels of monoSUMOylated condensin's kleisin Brn1 are reduced in the absence of Ulp2 compared with WT, while expression of a lysine-less SUMO variant *KRall* restores them (in two independent experiments). Ni PD was performed to isolate SUMO conjugates from cells expressing C-terminally 6HA-tagged Brn1.

See also Figure S6.

of $^{His}$SUMO (Figure 7E). This indicates that in the absence of Ulp2, SUMO chains might target the Smc5/6 complex for disassembly and release from chromatin, as observed for condensin.

## DISCUSSION

Genetic links between the SUMO protease Ulp2 and components of both condensin (Strunnikov et al., 2001) and cohesin (Stead et al., 2003) have been known for two decades, yet the role of Ulp2 in the regulation of these SMC complexes has remained elusive. Here, we uncover that Ulp2 acts as a guardian of all three SMC complexes by protecting them from unscheduled SUMO-chain-targeted turnover, thus giving them time to fulfill their functions on chromatin.

Specifically, using an unbiased SILAC-based proteomic screen to identify SUMO conjugates that decrease in abundance in the absence of Ulp2 in a SUMO-chain-dependent manner, we found subunits of all SMC complexes (Figure 1). Because *ULP2* overexpression was initially found to suppress phenotypes of *pds5-1* (Stead et al., 2003), we hypothesized that one important role of Pds5 is to recruit Ulp2 to protect cohesin from polySUMOylation. Strikingly, we showed that Pds5 not only binds Ulp2 (Figure S1), but that the essential role of Pds5 is to counteract SUMO chain formation, because *pds5*Δ lethality is suppressed by expressing a lysine-less SUMO variant (*KRall*) that cannot form SUMO chains (Figure 2B). Moreover, we found that this essential function of Pds5 can by bypassed by combined loss of *ELG1* and *WPL1* (Figure 2C), individual deletions of which suppress cohesion and condensation defects of *pds5-1*, respectively (Tong and Skibbens, 2015). Notably, the viability of *pds5*Δ *elg1*Δ *wpl1*Δ cells relies on Ulp2 (Figure 2F) or could be supported in its absence by expressing the *ulp1-C376* spontaneous suppressor of *ulp2*Δ phenotypes (Figure 2G), which gains ability to deSUMOylate Ulp2 substrates. We then uncovered that cohesin's kleisin Scc1 is in fact a Ulp2 substrate, and loss of Pds5 induces its polySUMOylation and subsequent degradation (Figure 3). Finally, we found that fusion of catalytically active Ulp2 to Scc1 suppresses the lethality of cells upon Pds5 loss. Furthermore, Scc1-Ulp2 fusion rescues the lethality of *pds5*Δ *elg1*Δ *wpl1*Δ mutant upon Ulp2 depletion and prevents polySUMOylation-targeted degradation of cohesin's kleisin (Figures 4 and 5). Thus, our data reveal that Ulp2 guards functional mono/multiSUMOylated cohesin pool loaded onto DNA (Almedawar et al., 2012; McAleenan et al., 2012) against unscheduled SUMO-chain-mediated turnover, providing the time window for its action until cohesin presence is no longer required, e.g., in mitosis to allow sister chromatid separation.

Interestingly, Ulp2 interacts with and is negatively regulated by the Polo-like kinase Cdc5 in mitosis, with impact on cohesion (Baldwin et al., 2009). *CDC5* overexpression causes centromeric cohesion defects that are suppressed by additionally overexpressing *ULP2*. Moreover, *CDC5* overexpression results in Pds5 dissociation from mitotic chromosomes in pre-anaphase cells, whereas co-overexpression of *ULP2* restores normal Pds5 chromosomal association (Baldwin et al., 2009). These findings suggest that Cdc5-mediated inactivation of Ulp2 induces SUMO-chain-targeted and Slx5/8 STUbL-mediated proteasomal degradation of the chromatin-bound mono/multiSUMOylated cohesin pool, ensuring its timely removal from chromosomes in collaboration with separase. Thus, yeast Cdc5 kinase promotes sister chromatid separation by phosphorylating Scc1 to enhance separase-mediated cleavage (Alexandru et al., 2001), and in parallel, by inducing SUMO-chain-mediated cohesin turnover through inactivation of Ulp2. Supporting this model, overexpression of *ULP2* in separase mutant *esp1-1* results in synthetic sick genetic interaction even at permissive temperatures for *esp1-1* (D'Ambrosio and Lavoie, 2014).

If the essential function of Pds5 is to help counteract polySUMOylation of cohesin mediated by Ulp2, why is deletion

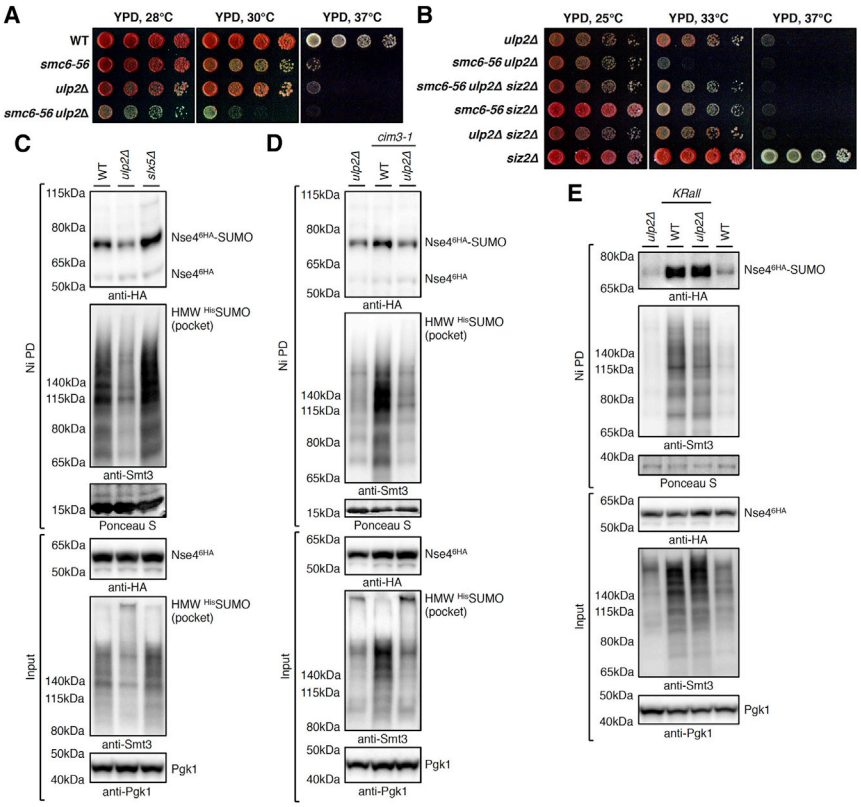


**Figure 7. The Smc5/6 complex is protected by Ulp2 against SUMO-chain-mediated turnover**

(A) Temperature-sensitive *smc6-56* mutant exhibits synthetic sick/lethal genetic interaction with *ulp2*Δ at permissive temperatures for *smc6-56* cells.

(B) Synthetic lethality of *smc6-56 ulp2*Δ cells at permissive temperatures for *smc6-56* single mutant is suppressed by deletion of the SUMO ligase Siz2.

(C) Levels of monoSUMOylated Smc5/6 complex kleisin Nse4 are reduced in the absence of Ulp2 compared with WT and increased upon Slx5 deletion (in two independent experiments). Ni PD was performed to isolate $^{His}$SUMO conjugates from cells expressing C-terminally 6HA-tagged Nse4.

(D) MonoSUMOylated Nse4 species are not degradation prone because they are not accumulating in the proteasome-defective *cim3-1* mutant (in two independent experiments).

(E) Expression of a chainless SUMO variant *KRall* leads to the accumulation of monoSUMOylated Nse4 species in both WT and *ulp2*Δ cells (in two independent experiments).

See also Figure S7.

of *PDS5* lethal, whereas *ulp2*Δ cells are viable? The presence of Ulp2, however, becomes essential in the *pds5*Δ mutant, when its lethality is bypassed by *elg1*Δ *wpl1*Δ (Figure 2F). We explain this by the overall structural organization of the SMC complexes (Nasmyth and Haering, 2005; Yatskevich et al., 2019) and of cohesin in particular (Hons et al., 2016; Shi et al., 2020), and by the promiscuity of the SUMOylation enzymes (Jentsch and Psakhye, 2013). Specifically, the SUMO conjugating enzyme Ubc9 efficiently targets any accessible lysine able to enter its active site *in vitro* without additional requirements of SUMO ligases. This feature makes the highly unstructured kleisin with many exposed lysines a perfect substrate for SUMOylation, unless it is bound by structured kleisin-associated regulatory subunits. In fact, human Scc1 is SUMOylated at multiple sites, and mutation of 15 lysines to arginines reduces, but does not abolish, its SUMOylation (Wu et al., 2012), whereas yeast Scc1 is multiSUMOylated on at least 11 lysines (McAleenan et al., 2012). The deletion of *PDS5* has a number of consequences for cohesin. First, Scc2-mediated cohesin DNA loading is strongly stimulated because there is no Pds5 to antagonize it (Petela et al., 2018) bringing more cohesin complexes in the vicinity of the DNA-bound SUMO ligases. Second, polySUMOylation at multiple acceptor sites on Scc1 is induced, because Pds5 is no longer available to bind Scc1, whereas Scc2 interaction with Scc1 is likely very dynamic as proposed previously (Petela et al., 2018). In the above-mentioned study, the authors fail to detect an increase in Scc2 association with the genome upon Pds5 depletion and speculate that Scc2 turnover is too rapid for efficient formaldehyde fixation. Because Scc1 is a highly unstructured protein, its exposed lysines can be readily targeted by the rather promiscuous SUMO conjugation machinery, if not shielded by Pds5. Third, loss of Pds5 abolishes recruitment of its interactors, including the SUMO protease Ulp2, to cohesin. Altogether, loss of Pds5 leads to increased Scc2-mediated DNA loading of cohesin with subsequent polySUMOylation and STUbL-mediated proteasomal degradation, exhausting the available pools of the unmodified Scc1. We show that SUMO chain build-up and kleisin turnover can be prevented if Ulp2 is fused to Scc1 (Figures 4 and 5), providing viability to cells lacking Pds5.

The suppression of the *pds5*Δ mutant lethality by *elg1*Δ *wpl1*Δ, where polySUMOylation of kleisin still takes place and the presence of Ulp2 is required to antagonize it and support viability, indicates that *elg1*Δ *wpl1*Δ-associated suppression is achieved by increasing the amounts of cohesin loaded onto DNA rather than by directly antagonizing polySUMOylation. Wpl1 is a cohesin release factor (Kueng et al., 2006), whereas Elg1 unloads PCNA, which is important for recruiting Eco1 to replication forks to promote cohesion during S phase (Moldovan et al., 2006). Interestingly, *ECO1* overexpression suppresses *pds5-1* temperature sensitivity (Noble et al., 2006), probably via Eco1-mediated Smc3 acetylation that antagonizes Wpl1-mediated cohesin release (Rolef Ben-Shahar et al., 2008; Unal et al., 2008). The increase of cohesin DNA loading provided by *elg1*Δ *wpl1*Δ is likely restricted to specific loci in yeast, because we did not observe pronounced increase in the Eco1-mediated Smc3 lysine K112, K113 acetylation in *elg1*Δ *wpl1*Δ cells compared with WT (Figure 2D; Figure S2C). However, this mild increase in cohesin is sufficient to support viability of *pds5Δ elg1*Δ *wpl1*Δ cells.

Deletion of Wpl1 in cells blocked in late G1 was previously shown to cause a major increase specifically in peri-centric cohesin, as monitored by Scc1 chromatin binding (Petela et al., 2018), whereas conditional depletion of Pds5-AID increased Scc2-mediated cohesin loading throughout the genome 2-fold. Interestingly, in line with the above-mentioned findings, we observed statistically significant increase of Scc1 association in *wpl1*Δ and *elg1*Δ *wpl1*Δ mutants compared with WT specifically at the pericentromeric region, but not at the chromosome arm in nocodazole-arrested cells (Figures S2D and S2E), which suggests that *elg1*Δ *wpl1*Δ might provide viability to *pds5*Δ cells by supporting pericentromeric cohesion. Moreover, we also observed a 2-fold increase in Scc1 loading at the centromere-distal region in nocodazole-arrested *elg1*Δ *wpl1*Δ *pds5*Δ mutant compared with WT and *elg1*Δ *wpl1*Δ cells (Figure S2E). Interestingly, increased topological DNA association of cohesin in nocodazole-arrested *pds5-101* cells shifted to restrictive temperature compared with WT cells was reported previously (Srinivasan et al., 2018), as monitored by the accumulation of monomeric supercoiled DNAs (CMs) in a minichromosome assay. Importantly, however, the authors observed in *pds5-101* cells a marked reduction in the accumulation of DNA-DNA concatemers (CDs) that mediate chromatid cohesion by co-entrapment of sister DNAs inside cohesin rings. Thus, despite having increased Scc2-mediated cohesin DNA loading, loss of Pds5 results in decreased Smc3 acetylation levels (Figure 2D; Figure S2C), loss of sister chromatid cohesion as monitored by minichromosome assay (Srinivasan et al., 2018), and cell lethality. In our work, we demonstrate that the lethality of *pds5*Δ cells is suppressed by expression of a SUMO variant unable to form chains (Figure 2B) or by fusing the SUMO protease Ulp2 that trims SUMO chains to the cohesin's kleisin Scc1 (Figures 4B and 4C). The fusion of catalytically active Ulp2 to Scc1 prevents its polySUMOylation and subsequent Scc1 kleisin turnover via proteasomal degradation (Figure 5), providing viability to cells lacking Pds5.

Similar to cohesin, Ulp2 guards the other two SMC complexes, condensin and the Smc5/6 complex, protecting them from SUMO-chain-targeted Slx5/8 STUbL-mediated turnover, as demonstrated by genetic interaction studies and the analysis of their kleisin SUMOylation in relevant mutants of the SUMO/ubiquitin pathway. The mechanism of Ulp2 action is similar, yet it likely results in preventing the disassembly and removal of the complexes from chromatin, rather than massive proteasomal degradation. Accordingly, monoSUMOylated species are not further enriched in the proteasome-defective *cim3-1* mutant but are nevertheless stabilized upon expression of the chainless SUMO variant *KRall*. Chromatin extraction of polySUMOylated and subsequently polyubiquitylated SMC complexes is likely mediated by the action of the Cdc48/p97 segregase (Dantuma and Hoppe, 2012; Franz et al., 2016), which was previously shown to mobilize cohesin and condensin from chromatin (Frattini et al., 2017; Thattikota et al., 2018). Despite this difference, the outcome of Ulp2 loss for all SMC complexes is the same in that their turnover on chromatin is increased. Another difference is that depletion of condensin's HAWKs or the KITE (kleisin-interacting tandem winged-helix element) proteins of the Smc5/6 complex is not suppressed by expressing the *KRall* SUMO mutant, suggesting that it is not their essential function to counteract kleisin polySUMOylation, contrary to Pds5. We note that Pds5 is likely a special case, because it is not stimulating the ATPase activity required for the DNA loading of cohesin, in contrast with the Scc2 HAWK, with which Pds5 competes and then replaces to stabilize the cohesin complex in the DNA-bound state (Petela et al., 2018).

In conclusion, here we uncovered that the SUMO protease Ulp2 acts on all three SMC complexes to protect them from unscheduled SUMO-chain-targeted turnover, giving them time to perform their essential functions on chromatin. Since Ulp2 discovery two decades ago (Li and Hochstrasser, 2000), multiple phenotypes have been associated with its loss, including genome instability, sister chromatid cohesion, and condensation defects. Our finding helps to explain many of them and highlights a SUMO-chain-governed layer of the SMC complex regulation, through which their chromatin abundance is instructed.

## STAR★METHODS

Detailed methods are provided in the online version of this paper and include the following:

- KEY RESOURCES TABLE
- RESOURCE AVAILABILITY
  - Lead contact
  - Materials availability
  - Data and code availability
- EXPERIMENTAL MODEL AND SUBJECT DETAILS
  - Yeast Strains
- METHOD DETAILS
  - Yeast Techniques
  - TCA Protein Precipitation
  - Ni-NTA Pull-down of $^{His}$SUMO Conjugates
  - Immunoprecipitation
  - ChIP-qPCR
  - Chromatin Fractionation
  - Mass Spectrometry
- QUANTIFICATION AND STATISTICAL ANALYSIS

## SUPPLEMENTAL INFORMATION

Supplemental information can be found online at https://doi.org/10.1016/j.celrep.2021.109485.

## ACKNOWLEDGMENTS

We thank Eurofins Genomics for WGS and analysis; M. Foiani, S. Jentsch, and K. Shirahige for reagents; A. Cattaneo and A. Bachi for mass spectrometry analysis; L. Fendillo for technical help; and R. Kawasumi for discussions. This work was supported by the Italian Association for Cancer Research (IG 23710), European Research Council (Consolidator Grant 682190 to D.B.), EMBO long-term fellowship (ALTF 561-2014), and an AIRC/Marie Curie Actions - COFUND iCARE fellowship (to I.P.). Funding for open access charge: European Research Council (Consolidator Grant 682190).

## AUTHOR CONTRIBUTIONS

I.P. and D.B. designed the study, analyzed the data, and wrote the paper. I.P. conducted the experiments.

## DECLARATION OF INTERESTS

The authors declare no competing interests.

Received: April 6, 2021
Revised: June 7, 2021
Accepted: July 7, 2021
Published: August 3, 2021

## REFERENCES

Alexandru, G., Uhlmann, F., Mechtler, K., Poupart, M.A., and Nasmyth, K. (2001). Phosphorylation of the cohesin subunit Scc1 by Polo/Cdc5 kinase regulates sister chromatid separation in yeast. Cell *105*, 459–472.

Almedawar, S., Colomina, N., Bermúdez-López, M., Pociño-Merino, I., and Torres-Rosell, J. (2012). A SUMO-dependent step during establishment of sister chromatid cohesion. Curr. Biol. *22*, 1576–1581.

Baldwin, M.L., Julius, J.A., Tang, X., Wang, Y., and Bachant, J. (2009). The yeast SUMO isopeptidase Smt4/Ulp2 and the polo kinase Cdc5 act in an opposing fashion to regulate sumoylation in mitosis and cohesion at centromeres. Cell Cycle *8*, 3406–3419.

Borges, V., Lehane, C., Lopez-Serra, L., Flynn, H., Skehel, M., Rolef Ben-Shahar, T., and Uhlmann, F. (2010). Hos1 deacetylates Smc3 to close the cohesin acetylation cycle. Mol. Cell *39*, 677–688.

Branzei, D., Sollier, J., Liberi, G., Zhao, X., Maeda, D., Seki, M., Enomoto, T., Ohta, K., and Foiani, M. (2006). Ubc9- and mms21-mediated sumoylation counteracts recombinogenic events at damaged replication forks. Cell *127*, 509–522.

Bustard, D.E., Ball, L.G., and Cobb, J.A. (2016). Non-Smc element 5 (Nse5) of the Smc5/6 complex interacts with SUMO pathway components. Biol. Open *5*, 777–785.

Ciosk, R., Shirayama, M., Shevchenko, A., Tanaka, T., Toth, A., Shevchenko, A., and Nasmyth, K. (2000). Cohesin's binding to chromosomes depends on a separate complex consisting of Scc2 and Scc4 proteins. Mol. Cell *5*, 243–254.

Cox, J., and Mann, M. (2008). MaxQuant enables high peptide identification rates, individualized p.p.b.-range mass accuracies and proteome-wide protein quantification. Nat. Biotechnol. *26*, 1367–1372.

D'Ambrosio, L.M., and Lavoie, B.D. (2014). Pds5 prevents the PolySUMO-dependent separation of sister chromatids. Curr. Biol. *24*, 361–371.

D'Amours, D., Stegmeier, F., and Amon, A. (2004). Cdc14 and condensin control the dissolution of cohesin-independent chromosome linkages at repeated DNA. Cell *117*, 455–469.

Dantuma, N.P., and Hoppe, T. (2012). Growing sphere of influence: Cdc48/p97 orchestrates ubiquitin-dependent extraction from chromatin. Trends Cell Biol. *22*, 483–491.

Dorsett, D. (2011). Cohesin: genomic insights into controlling gene transcription and development. Curr. Opin. Genet. Dev. *21*, 199–206.

Eckhoff, J., and Dohmen, R.J. (2015). In vitro studies reveal a sequential mode of chain processing by the yeast SUMO (Small Ubiquitin-related Modifier)-specific protease Ulp2. J. Biol. Chem. *290*, 12268–12281.

Elmore, Z.C., Donaher, M., Matson, B.C., Murphy, H., Westerbeck, J.W., and Kerscher, O. (2011). Sumo-dependent substrate targeting of the SUMO protease Ulp1. BMC Biol. *9*, 74.

Flotho, A., and Melchior, F. (2013). Sumoylation: a regulatory protein modification in health and disease. Annu. Rev. Biochem. *82*, 357–385.

Franz, A., Ackermann, L., and Hoppe, T. (2016). Ring of change: CDC48/p97 drives protein dynamics at chromatin. Front. Genet. *7*, 73.

Frattini, C., Villa-Hernández, S., Pellicanò, G., Jossen, R., Katou, Y., Shirahige, K., and Bermejo, R. (2017). Cohesin ubiquitylation and mobilization facilitate stalled replication fork dynamics. Mol. Cell *68*, 758–772.e4.

Hartman, T., Stead, K., Koshland, D., and Guacci, V. (2000). Pds5p is an essential chromosomal protein required for both sister chromatid cohesion and condensation in Saccharomyces cerevisiae. J. Cell Biol. *151*, 613–626.

Hickey, C.M., Wilson, N.R., and Hochstrasser, M. (2012). Function and regulation of SUMO proteases. Nat. Rev. Mol. Cell Biol. *13*, 755–766.

Hons, M.T., Huis In 't Veld, P.J., Kaesler, J., Rombaut, P., Schleiffer, A., Herzog, F., Stark, H., and Peters, J.M. (2016). Topology and structure of an engineered human cohesin complex bound to Pds5B. Nat. Commun. *7*, 12523.

James, P., Halladay, J., and Craig, E.A. (1996). Genomic libraries and a host strain designed for highly efficient two-hybrid selection in yeast. Genetics *144*, 1425–1436.

Janke, C., Magiera, M.M., Rathfelder, N., Taxis, C., Reber, S., Maekawa, H., Moreno-Borchart, A., Doenges, G., Schwob, E., Schiebel, E., and Knop, M. (2004). A versatile toolbox for PCR-based tagging of yeast genes: new fluorescent proteins, more markers and promoter substitution cassettes. Yeast *21*, 947–962.

Jentsch, S., and Psakhye, I. (2013). Control of nuclear activities by substrate-selective and protein-group SUMOylation. Annu. Rev. Genet. *47*, 167–186.

Kubota, T., Nishimura, K., Kanemaki, M.T., and Donaldson, A.D. (2013). The Elg1 replication factor C-like complex functions in PCNA unloading during DNA replication. Mol. Cell *50*, 273–280.

Kueng, S., Hegemann, B., Peters, B.H., Lipp, J.J., Schleiffer, A., Mechtler, K., and Peters, J.M. (2006). Wapl controls the dynamic association of cohesin with chromatin. Cell *127*, 955–967.

Ladurner, R., Bhaskara, V., Huis in 't Veld, P.J., Davidson, I.F., Kreidl, E., Petzold, G., and Peters, J.M. (2014). Cohesin's ATPase activity couples cohesin loading onto DNA with Smc3 acetylation. Curr. Biol. *24*, 2228–2237.

Li, S.J., and Hochstrasser, M. (1999). A new protease required for cell-cycle progression in yeast. Nature *398*, 246–251.

Li, S.J., and Hochstrasser, M. (2000). The yeast ULP2 (SMT4) gene encodes a novel protease specific for the ubiquitin-like Smt3 protein. Mol. Cell. Biol. *20*, 2367–2377.

Li, S.J., and Hochstrasser, M. (2003). The Ulp1 SUMO isopeptidase: distinct domains required for viability, nuclear envelope localization, and substrate specificity. J. Cell Biol. *160*, 1069–1081.

Li, Y., Muir, K.W., Bowler, M.W., Metz, J., Haering, C.H., and Panne, D. (2018). Structural basis for Scc3-dependent cohesin recruitment to chromatin. eLife *7*, e38356.

Liang, J., Singh, N., Carlson, C.R., Albuquerque, C.P., Corbett, K.D., and Zhou, H. (2017). Recruitment of a SUMO isopeptidase to rDNA stabilizes silencing complexes by opposing SUMO targeted ubiquitin ligase activity. Genes Dev. *31*, 802–815.

Losada, A. (2014). Cohesin in cancer: chromosome segregation and beyond. Nat. Rev. Cancer *14*, 389–393.

Mann, M. (2006). Functional and quantitative proteomics using SILAC. Nat. Rev. Mol. Cell Biol. *7*, 952–958.

Maradeo, M.E., and Skibbens, R.V. (2010). Replication factor C complexes play unique pro- and anti-establishment roles in sister chromatid cohesion. PLoS ONE *5*, e15381.

McAleenan, A., Cordon-Preciado, V., Clemente-Blanco, A., Liu, I.C., Sen, N., Leonard, J., Jarmuz, A., and Aragón, L. (2012). SUMOylation of the α-kleisin subunit of cohesin is required for DNA damage-induced cohesion. Curr. Biol. *22*, 1564–1575.

Menolfi, D., Delamarre, A., Lengronne, A., Pasero, P., and Branzei, D. (2015). Essential roles of the Smc5/6 complex in replication through natural pausing sites and endogenous DNA damage tolerance. Mol. Cell *60*, 835–846.

Moldovan, G.L., Pfander, B., and Jentsch, S. (2006). PCNA controls establishment of sister chromatid cohesion during S phase. Mol. Cell *23*, 723–732.

Mossessova, E., and Lima, C.D. (2000). Ulp1-SUMO crystal structure and genetic analysis reveal conserved interactions and a regulatory element essential for cell growth in yeast. Mol. Cell *5*, 865–876.

Mullen, J.R., Das, M., and Brill, S.J. (2011). Genetic evidence that polysumoylation bypasses the need for a SUMO-targeted Ub ligase. Genetics *187*, 73–87.

Nasmyth, K., and Haering, C.H. (2005). The structure and function of SMC and kleisin complexes. Annu. Rev. Biochem. *74*, 595–648.

Nasmyth, K., and Haering, C.H. (2009). Cohesin: its roles and mechanisms. Annu. Rev. Genet. *43*, 525–558.

Nishimura, K., Fukagawa, T., Takisawa, H., Kakimoto, T., and Kanemaki, M. (2009). An auxin-based degron system for the rapid depletion of proteins in nonplant cells. Nat. Methods *6*, 917–922.

Noble, D., Kenna, M.A., Dix, M., Skibbens, R.V., Unal, E., and Guacci, V. (2006). Intersection between the regulators of sister chromatid cohesion establishment and maintenance in budding yeast indicates a multi-step mechanism. Cell Cycle *5*, 2528–2536.

Panizza, S., Tanaka, T., Hochwagen, A., Eisenhaber, F., and Nasmyth, K. (2000). Pds5 cooperates with cohesin in maintaining sister chromatid cohesion. Curr. Biol. *10*, 1557–1564.

Panse, V.G., Küster, B., Gerstberger, T., and Hurt, E. (2003). Unconventional tethering of Ulp1 to the transport channel of the nuclear pore complex by karyopherins. Nat. Cell Biol. *5*, 21–27.

Perez-Riverol, Y., Csordas, A., Bai, J., Bernal-Llinares, M., Hewapathirana, S., Kundu, D.J., Inuganti, A., Griss, J., Mayer, G., Eisenacher, M., et al. (2019). The PRIDE database and related tools and resources in 2019: improving support for quantification data. Nucleic Acids Res. *47* (*D1*), D442–D450.

Petela, N.J., Gligoris, T.G., Metson, J., Lee, B.G., Voulgaris, M., Hu, B., Kikuchi, S., Chapard, C., Chen, W., Rajendra, E., et al. (2018). Scc2 is a potent activator of cohesin's ATPase that promotes loading by binding Scc1 without Pds5. Mol. Cell *70*, 1134–1148.e7.

Potts, P.R., Porteus, M.H., and Yu, H. (2006). Human SMC5/6 complex promotes sister chromatid homologous recombination by recruiting the SMC1/3 cohesin complex to double-strand breaks. EMBO J. *25*, 3377–3388.

Psakhye, I., and Jentsch, S. (2012). Protein group modification and synergy in the SUMO pathway as exemplified in DNA repair. Cell *151*, 807–820.

Psakhye, I., and Jentsch, S. (2016). Identification of substrates of protein-group SUMOylation. Methods Mol. Biol. *1475*, 219–231.

Psakhye, I., Castellucci, F., and Branzei, D. (2019). SUMO-chain-regulated proteasomal degradation timing exemplified in DNA replication initiation. Mol. Cell *76*, 632–645.e6.

Robellet, X., Fauque, L., Legros, P., Mollereau, E., Janczarski, S., Parrinello, H., Desvignes, J.P., Thevenin, M., and Bernard, P. (2014). A genetic screen for functional partners of condensin in fission yeast. G3 (Bethesda) *4*, 373–381.

Robinson, J.T., Thorvaldsdóttir, H., Winckler, W., Guttman, M., Lander, E.S., Getz, G., and Mesirov, J.P. (2011). Integrative genomics viewer. Nat. Biotechnol. *29*, 24–26.

Rolef Ben-Shahar, T., Heeger, S., Lehane, C., East, P., Flynn, H., Skehel, M., and Uhlmann, F. (2008). Eco1-dependent cohesin acetylation during establishment of sister chromatid cohesion. Science *321*, 563–566.

Sherman, F. (1991). Getting started with yeast. Methods Enzymol. *194*, 3–21.

Shi, Z., Gao, H., Bai, X.C., and Yu, H. (2020). Cryo-EM structure of the human cohesin-NIPBL-DNA complex. Science *368*, 1454–1459.

Sollier, J., Driscoll, R., Castellucci, F., Foiani, M., Jackson, S.P., and Branzei, D. (2009). The Saccharomyces cerevisiae Esc2 and Smc5-6 proteins promote sister chromatid junction-mediated intra-S repair. Mol. Biol. Cell *20*, 1671–1682.

Srinivasan, M., Scheinost, J.C., Petela, N.J., Gligoris, T.G., Wissler, M., Ogushi, S., Collier, J.E., Voulgaris, M., Kurze, A., Chan, K.L., et al. (2018). The cohesin ring uses its hinge to organize DNA using non-topological as well as topological mechanisms. Cell *173*, 1508–1519.e18.

Sriramachandran, A.M., and Dohmen, R.J. (2014). SUMO-targeted ubiquitin ligases. Biochim. Biophys. Acta *1843*, 75–85.

Stead, K., Aguilar, C., Hartman, T., Drexel, M., Meluh, P., and Guacci, V. (2003). Pds5p regulates the maintenance of sister chromatid cohesion and is sumoylated to promote the dissolution of cohesion. J. Cell Biol. *163*, 729–741.

Strunnikov, A.V., Aravind, L., and Koonin, E.V. (2001). Saccharomyces cerevisiae SMT4 encodes an evolutionarily conserved protease with a role in chromosome condensation regulation. Genetics *158*, 95–107.

Suhandynata, R.T., Quan, Y., Yang, Y., Yuan, W.T., Albuquerque, C.P., and Zhou, H. (2019). Recruitment of the Ulp2 protease to the inner kinetochore prevents its hyper-sumoylation to ensure accurate chromosome segregation. PLoS Genet. *15*, e1008477.

Takahashi, Y., Dulev, S., Liu, X., Hiller, N.J., Zhao, X., and Strunnikov, A. (2008). Cooperation of sumoylated chromosomal proteins in rDNA maintenance. PLoS Genet. *4*, e1000215.

Thattikota, Y., Tollis, S., Palou, R., Vinet, J., Tyers, M., and D'Amours, D. (2018). Cdc48/VCP promotes chromosome morphogenesis by releasing condensin from self-entrapment in chromatin. Mol. Cell *69*, 664–676.e5.

Tong, K., and Skibbens, R.V. (2015). Pds5 regulators segregate cohesion and condensation pathways in Saccharomyces cerevisiae. Proc. Natl. Acad. Sci. USA *112*, 7021–7026.

Unal, E., Heidinger-Pauli, J.M., Kim, W., Guacci, V., Onn, I., Gygi, S.P., and Koshland, D.E. (2008). A molecular determinant for the establishment of sister chromatid cohesion. Science *321*, 566–569.

Wagner, K., Kunz, K., Piller, T., Tascher, G., Hölper, S., Stehmeier, P., Keiten-Schmitz, J., Schick, M., Keller, U., and Müller, S. (2019). The SUMO isopeptidase SENP6 functions as a rheostat of chromatin residency in genome maintenance and chromosome dynamics. Cell Rep. *29*, 480–494.e5.

Wu, N., Kong, X., Ji, Z., Zeng, W., Potts, P.R., Yokomori, K., and Yu, H. (2012). Scc1 sumoylation by Mms21 promotes sister chromatid recombination through counteracting Wapl. Genes Dev. *26*, 1473–1485.

Xu, X., and Yanagida, M. (2019). Suppressor screening reveals common kleisin-hinge interaction in condensin and cohesin, but different modes of regulation. Proc. Natl. Acad. Sci. USA *116*, 10889–10898.

Yatskevich, S., Rhodes, J., and Nasmyth, K. (2019). Organization of Chromosomal DNA by SMC Complexes. Annu. Rev. Genet. *53*, 445–482.

Zhao, X., and Blobel, G. (2005). A SUMO ligase is part of a nuclear multiprotein complex that affects DNA repair and chromosomal organization. Proc. Natl. Acad. Sci. USA *102*, 4777–4782.

## STAR★METHODS

### KEY RESOURCES TABLE

| REAGENT or RESOURCE | SOURCE | IDENTIFIER |
|---|---|---|
| **Antibodies** | | |
| Mouse monoclonal anti-Viral V5-TAG antibody (clone SV5-Pk1) (Dilution for western blot 1:5000) | Bio-Rad / AbD Serotec | Cat# MCA1360; RRID: AB_322378 |
| Mouse monoclonal anti-Pgk1 antibody (clone 22C5D8) (Dilution for western blot 1:2000) | Thermo Fisher Scientific | Cat# 459250; RRID: AB_2532235 |
| Mouse monoclonal anti c-MYC antibody (clone 9E10) (Dilution for western blot 1:2000) | In house | N/A |
| Mouse monoclonal anti-HA (F-7) antibody (Dilution for western blot 1:2000) | Santa Cruz Biotechnology | Cat# sc-7392; RRID: AB_627809 |
| Rabbit polyclonal anti-Smt3 (y-84) antibody (Dilution for western blot 1:2000) | Santa Cruz Biotechnology | Cat# sc-28649; RRID: AB_661135 |
| Mouse monoclonal anti-acetyl-Smc3 antibody (Dilution for western blot 1:2000) | Gift from Katsuhiko Shirahige (Borges et al., 2010) | N/A |
| Rabbit polyclonal anti-Histone H4 antibody (Dilution for western blot 1:2000) | Abcam | Cat# ab7311, RRID: AB_305837 |
| Anti-rabbit IgG, HRP-linked antibody (Dilution for western blot 1:5000) | Cell Signaling Technology | Cat# 7074; RRID: AB_2099233 |
| Anti-mouse IgG, HRP-linked antibody (Dilution for western blot 1:5000) | Cell Signaling Technology | Cat# 7076; RRID: AB_330924 |
| Normal mouse IgG | Santa Cruz Biotechnology | Cat# sc-2025; RRID: AB_737182 |
| **Chemicals, peptides, and recombinant proteins** | | |
| Imidazole | Sigma-Aldrich | Cat# I2399 |
| Hydroxyurea (HU) | Sigma-Aldrich | Cat# H8627 |
| 3-Amino-triazole (3-AT) | Sigma-Aldrich | Cat# A8056 |
| Benomyl | Sigma-Aldrich | Cat# 45339 |
| Camptothecin (CPT) | Sigma-Aldrich | Cat# C9911 |
| Methyl methanesulfonate (MMS) | Sigma-Aldrich | Cat# 129925 |
| 3-Indole acetic acid (IAA) | Abcam | Cat# ab146402 |
| Ni-NTA agarose | QIAGEN | Cat# 30210 |
| Recombinant protein G – Sepharose 4B | Thermo Fisher Scientific | Cat# 101243 |
| cOmplete, EDTA-free protease inhibitor cocktail tablets | Roche | Cat# 4693132001 |
| N-Ethylmaleimide | Sigma-Aldrich | Cat# E3876 |
| Phenylmethanesulfonyl fluoride | Sigma-Aldrich | Cat# P7626 |
| Iodoacetamide | Sigma-Aldrich | Cat# I1149 |
| Phosphatase inhibitor cocktail 2 | Sigma-Aldrich | Cat# P5726 |
| Phosphatase inhibitor cocktail 3 | Sigma-Aldrich | Cat# P0044 |
| Zymolyase 100T (Arthrobacter luteus) | Seikagaku Corporation | Cat# 120493 |
| Ribonuclease A from bovine pancreas | Sigma-Aldrich | Cat# R5503 |
| Proteinase K, recombinant, PCR Grade | Roche | Cat# 03115801001 |
| **Critical commercial assays** | | |
| Invitrogen Bolt 4-12% Bis-Tris Plus Gels, 15-well | Thermo Fisher Scientific | Cat# NW04125BOX |
| Genomic-tip 100/G | QIAGEN | Cat# 10243 |
| QIAquick PCR purification kit | QIAGEN | Cat# 28106 |

(*Continued on next page*)

*Continued*

| REAGENT or RESOURCE | SOURCE | IDENTIFIER |
|---|---|---|
| L-Arginine:HCl (U-13C6, 99%; U-15N4, 99%) | Cambridge Isotope Laboratories, Inc. | CAS# 1119-34-2 CNLM-539-H-0.25 |
| L-Lysine:2HCl (U-13C6, 99%; U-15N2, 99%) | Cambridge Isotope Laboratories, Inc. | CAS# 657-26-1 CNLM-291-H-0.25 |
| Deposited data | | |
| SILAC-based proteomic screen to detect degradation-prone SUMOylated substrates that decrease in abundance in a SUMO-chain-dependent manner in u*lp2*Δ *cim3-1* cells. | This paper | PXD022717 |
| Experimental models: Organisms/Strains | | |
| Saccharomyces cerevisiae strains used in this work, except those specifically indicated and Y2HGold strain used for yeast two-hybrid studies, are W303 background derivatives with the wild type *RAD5* locus. | This paper (see Table S1) | N/A |
| Y2HGold yeast strain | Takara | Cat# 630498 |
| Recombinant DNA | | |
| pGAD-C1, pGBD-C1 | James et al., 1996 | N/A |
| Software and algorithms | | |
| Integrative Genomics Viewer (IGV 2.3) | Robinson et al., 2011 | http://software.broadinstitute.org/software/igv/igv2.3 |
| MaxQuant (version 1.5.2.8) | Cox and Mann, 2008 | https://www.biochem.mpg.de/5111795/maxquant |
| Other | | |
| Illumina MiSeq v2 whole-genome sequencing | Eurofins Genomics | https://eurofinsgenomics.eu/ |

## RESOURCE AVAILABILITY

### Lead contact

Further information and requests for resources and reagents should be directed to and will be fulfilled by the Lead Contact, Dana Branzei (dana.branzei@ifom.eu).

### Materials availability

All unique reagents generated in this study are available from the Lead Contact with a completed Materials Transfer Agreement.

### Data and code availability

- The mass spectrometry proteomics data have been deposited to the ProteomeXchange Consortium via the PRIDE (Perez-Riverol et al., 2019) partner repository with the dataset identifier PXD022717. They are publicly available as of the date of publication. Accession number is also listed in the Key resources table.
- This study did not generate any code.
- Any additional information required to reanalyze the data reported in this paper is available from the Lead Contact upon request.

## EXPERIMENTAL MODEL AND SUBJECT DETAILS

### Yeast Strains

Chromosomally tagged *Saccharomyces cerevisiae* strains and mutants were constructed by a PCR-based strategy, by genetic crosses and standard techniques (Janke et al., 2004). Standard cloning and site-directed mutagenesis techniques were used. Strains and all genetic manipulations were verified by polymerase chain reaction (PCR), sequencing and phenotype. Maps and primer DNA sequences are available upon request. All yeast strains used in this work except those specifically indicated and used for the yeast two-hybrid (Y2H) studies are isogenic to W303 background and are listed in the Key resources table.

## METHOD DETAILS

### Yeast Techniques

Yeast cultures were inoculated from overnight cultures, grown using standard growth conditions and media (Sherman, 1991). All cultures were grown in YPD media containing glucose (2%) as carbon source at 28°C unless otherwise indicated. For the transcriptional shut-off of genes expressed under the control of *GAL* promoter, cells were grown in YP Gal media containing galactose (2%), washed once with 1X PBS and shifted to YPD media or plated on YPD plates. For drug sensitivity assays, cells from overnight cultures were counted and diluted before being spotted on YPD plates containing the indicated concentrations of drugs and incubated at 28°C for 2-3 days. For Y2H analysis catalytically-dead *ulp2-C624S* mutant and different truncations of *PDS5* were cloned into pGAD-C1 or pGBD-C1 vectors and cotransformed into Y2HGold yeast strain. Standard cloning and site-directed mutagenesis techniques were used. Maps and primer DNA sequences are available upon request.

### TCA Protein Precipitation

To preserve the post-translational modifications, yeast cells were lysed under denaturing conditions. For preparation of denatured protein extracts, yeast cultures grown to an $OD_{600}$ = 0.7-1 were pelleted by centrifugation (4000 rpm, 4 min, 4°C) and immediately frozen in liquid nitrogen. After thawing on ice, the pellets were lysed by addition of denaturing lysis buffer (1.85 M NaOH, 7.5% β-mercaptoethanol) for 15min on ice. For the cell pellet of an $OD_{600}$ = 1 typically 150 μL of lysis buffer was used. To precipitate the proteins, the lysate was subsequently mixed with an equal volume (150 μL in case of $OD_{600}$ = 1) of 55% (w/v) trichloroacetic acid (TCA) and further incubated on ice for 15 min. The precipitated material was recovered by two sequential centrifugation steps (13000 rpm, 4°C, 15 min). Pelleted denatured proteins were then either directly resuspended in HU sample buffer (8 M urea, 5% SDS, 1 mM EDTA, 1,5% DTT, 1% bromophenol blue; 50 μL per $OD_{600}$ = 1), boiled for 10 min and stored at −20°C, or used for downstream processing, e.g., Ni-NTA pull-downs of His-tagged SUMO conjugates.

### Ni-NTA Pull-down of $^{His}$SUMO Conjugates

For isolation of *in vivo* SUMOylated substrates from yeast cells expressing N-terminally His-tagged Smt3 ($^{His}$SUMO), denatured protein extracts were prepared and Ni-NTA chromatography was carried out as described previously (Psakhye and Jentsch, 2012, 2016). In general, 200 $OD_{600}$ = 1 of logarithmically growing cells were harvested by centrifugation (4000 rpm, 4 min, 4°C), washed with pre-chilled water, transferred to 50 mL falcon tube and lysed with 6 mL of 1.85 M NaOH / 7.5% β-mercaptoethanol for 15 min on ice. The proteins were precipitated by adding 6 mL of 55% TCA and another 15 min incubation on ice (TCA-precipitation, described above). Next, the precipitate was pelleted by centrifugation (3500 rpm, 15 min, 4°C), washed twice with water and finally resuspended in buffer A (6 M guanidine hydrochloride, 100 mM $NaH_2PO_4$, 10 mM Tris-HCl, pH 8.0, 20 mM imidazole) containing 0.05% Tween-20. After incubation for 1 hour on a roller at room temperature with subsequent removal of insoluble aggregates by centrifugation (23000 g, 20 min, 4°C), the protein solution was incubated overnight at 4°C with 50 μL of Ni-NTA agarose beads in the presence of 20 mM imidazole. After incubation, the beads were washed three times with buffer A containing 0.05% Tween-20 and five times with buffer B (8 M urea, 100 mM $NaH_2PO_4$, 10 mM Tris-HCl, pH 6.3) with 0.05% Tween-20. $^{His}$SUMO conjugates bound to the beads were finally eluted by incubation with 50 μL of HU sample buffer for 10 min at 65°C. Proteins were resolved on precast Bolt 4%–12% Bis-Tris Plus gradient gels, and analyzed by standard western blotting techniques using antibodies listed in the Key resources table.

### Immunoprecipitation

For the immunoprecipitation (IP) and binding studies involving co-IP, native yeast extracts were prepared by cell disruption using grinding in liquid nitrogen. To avoid protein degradation and loss of PTMs, lysis buffer (150 mM NaCl, 10% glycerol, 1% NP-40, 50 mM Tris HCl, pH 8.0) was supplemented with inhibitors: EDTA-free complete cocktail, 20 mM N-ethylmaleimide, 1 mM phenylmethanesulfonyl fluoride (PMSF), 25 mM iodoacetamide, and phosphatase inhibitor cocktails 2 and 3 (Sigma-Aldrich). For IPs, anti-PK and anti-MYC antibodies, together with recombinant protein G Sepharose 4B beads were used. IPs were performed overnight with head-over-tail rotation at 4°C and were followed by stringent washing steps to remove non-specific background binding to the beads.

### ChIP-qPCR

Chromatin immunoprecipitation (ChIP) was carried out as previously described (Psakhye et al., 2019). Briefly, cells were collected at the indicated experimental conditions and crosslinked with 1% formaldehyde for 30 min. Cells were washed twice with ice-cold 1X TBS, suspended in lysis buffer supplemented with 1 mM PMSF, 20 mM NEM, and 1X EDTA-free complete cocktail, and lysed using FastPrep-24 (MP Biomedicals). Chromatin was sheared to a size of 300-500 bp by sonication. IP reactions with anti-HA antibodies and Dynabeads protein G were allowed to proceed overnight at 4°C. After washing and eluting the ChIP fractions from beads, crosslinks were reversed at 65°C overnight for both Input and IP. After proteinase K treatment, DNA was extracted twice by phenol/chlorophorm/isoamyl alcohol (25:24:1, v/v). Following precipitation with ethanol and Ribonuclease A (RNase A) treatment, DNA was purified using QIAquick PCR purification kit. Real-time PCR was performed using QuantiFast SYBR Green PCR kit according to the manufacturer's instructions and each reaction was performed in triplicates using a Roche LightCycler 96 system.

The results were analyzed with absolute quantification/2nd derivative maximum and the 2(-ΔC(t)) method. Each ChIP experiment was repeated at least three times. Statistical analysis was performed using Student's unpaired t test. The error bars represent standard error of mean (SEM).

### Chromatin Fractionation

The chromatin binding assay was performed as described previously (Psakhye and Jentsch, 2012). Briefly, native yeast protein extract was prepared from 50 $OD_{600}$ = 1 of logarithmically growing culture by treating harvested cells with zymolyase (0.2 mg/ml) in spheroplast buffer (0.6 M Sorbitol, 10 mM DTT, 50 mM potassium phosphate buffer, pH 7.5) for 1 hour at 37°C to produce spheroplasts and disrupting them with 1% Triton X-100 in extraction buffer (100 mM KCl, 2.5 mM $MgCl_2$, 1 mM DTT, 50 mM HEPES-KOH, pH 7.5) supplemented with 1 mM PMSF, 20 mM NEM, and 1X EDTA-free complete cocktail. The resulting whole cell extract (WCE) was carefully applied on top of the 30% sucrose cushion of equal volume and centrifuged for 30 min at 20000 g at 4°C. The supernatant containing soluble protein fraction (SUP) was carefully collected from the top of the cushion, sucrose aspirated and the pellet containing the chromatin fraction (CHR) was resuspended in HU sample buffer for subsequent SDS-PAGE and western blot analysis.

### Mass Spectrometry

For the detection of degradation-prone SUMO conjugates decreased in abundance in *ulp2*Δ *cim3-1* mutant cells specifically in a SUMO-chain-dependent manner (Figure 1), SILAC-based mass spectrometry protocol (Mann, 2006) was used. Yeast *ulp2*Δ *cim3-1* mutant cells deficient in biosynthesis of lysine and arginine (*lys1*Δ and *arg4*Δ) expressing either wild-type His-tagged SUMO ($^{His}$SUMO) or its lysine-less variant (*KRall*) that cannot form lysine-linked polySUMO chains were grown for at least ten divisions in synthetic complete media supplemented either with unlabeled (Lys0 and Arg0; light) or heavy isotope-labeled amino acids (Lys8 and Arg10; heavy) from Cambridge Isotope Laboratories. Exponentially dividing $^{His}$*SUMO ulp2*Δ *cim3-1* cells grown in heavy media were harvested, combined with equal amount of *KRall ulp2*Δ *cim3-1* cells grown in light media, and SUMO conjugates were isolated by using denaturing Ni-NTA pull-down. Proteins isolated following denaturing Ni-NTA pull-downs of $^{His}$SUMO conjugates were separated on 4%–12% Bis-Tris gel and stained by Coomassie colloidal blue. The gel lane was cut into slices, each of which was reduced, alkylated, and digested with trypsin. Peptides mixtures were desalted and concentrated on a home-made $C_{18}$ desalting tip, and peptides were injected in a nano HPLC EasyLC (Proxeon Biosystems, Denmark). Peptides separation occurred onto a 25 cm long column, reverse phase spraying fused silica capillary column (75 μm i.d.) packed in house with 3 μm ReproSil AQ C18 (Dr. Maisch GmbH, Germany) resin. The LC system was connected to a Q Exactive-HF mass spectrometer (Thermo Fisher Scientific, Germany) equipped with a nanoelectrospray ion source (Proxeon Biosystems, Denmark). Identification and quantification of peptides and proteins was performed with MaxQuant (Cox and Mann, 2008) software. Criteria for identification of a protein were: at least two peptides (one unique) sequenced, six amino acids of minimal peptide length, FDR < 1%, and quantification achieved with at least two ratio counts.

## QUANTIFICATION AND STATISTICAL ANALYSIS

Three or more independent experiments were performed to obtain the data. Statistical analysis was performed using Student's unpaired t test. The error bars represent standard error of mean (SEM). The mean values ± SEM are plotted, whereas $p < 0.05$ and $p < 0.01$ are considered significant and expressed as * and **, respectively. The statistical details of experiments can be found in the figure legends.